AD________________

Award Number: DAMD17-02-1-0119

TITLE: Sodium Iodide Symporter Gene Transfer for Imaging and Ablation of Prostate Cancer

PRINCIPAL INVESTIGATOR: Sissy M. Jhiang, Ph.D.

CONTRACTING ORGANIZATION: The Ohio State University Research Foundation
Columbus, Ohio 43210-1063

REPORT DATE: January 2005

TYPE OF REPORT: Final

PREPARED FOR: U.S. Army Medical Research and Materiel Command
Fort Detrick, Maryland 21702-5012

REPORT DOCUMENTATION PAGE

Form Approved
OMB No. 074-0188

1. AGENCY USE ONLY (Leave blank)	2. REPORT DATE	3. REPORT TYPE AND DATES COVERED
	January 2005	Final (15 Dec 2001 - 14 Dec 2004)

4. TITLE AND SUBTITLE
Sodium Iodide Symporter Gene Transfer for Imaging and Ablation of Prostate Cancer

5. FUNDING NUMBERS
DAMD17-02-1-0119

6. AUTHOR(S)
Sissy M. Jhiang, Ph.D.

7. PERFORMING ORGANIZATION NAME(S) AND ADDRESS(ES)
The Ohio State University Research Foundation
Columbus, Ohio 43210-1063

E-Mail: Jhiang.1@osu.edu

8. PERFORMING ORGANIZATION REPORT NUMBER

9. SPONSORING / MONITORING AGENCY NAME(S) AND ADDRESS(ES)
U.S. Army Medical Research and Materiel Command
Fort Detrick, Maryland 21702-5012

10. SPONSORING / MONITORING AGENCY REPORT NUMBER

11. SUPPLEMENTARY NOTES

12a. DISTRIBUTION / AVAILABILITY STATEMENT
Approved for Public Release; Distribution Unlimited

12b. DISTRIBUTION CODE

13. ABSTRACT (Maximum 200 Words)

The sodium iodide symporter (NIS) mediates iodide uptake in thyroid follicular cells and provides a mechanism for effective radioiodide treatment of residual, recurrent, and metastatic thyroid cancers. The objective of the proposed research is to test the hypothesis that expression of exogenous hNIS in prostatic tissue will enable radioiodide to localize and ablate residual prostate cancer following prostatectomy, such that recurrence and metastasis of the disease can be prevented. The specific aims of this project are to: (1) confirm metastatic progression to distant lymph nodes and lungs following subcutaneous inoculation of rats with MATLyLu prostatic adenocarcinoma cells expressing hNIS; (2) investigate whether radioiodide therapy will prevent metastases and/or prolong survival in rats bearing subcutaneous MATLyLu tumors that express hNIS; (3) determine the expression level of hNIS required to elicit selective radioiodide-mediated killing of MATLyLu-hNIS prostatic adenocarcinoma cells *in vivo*; and, (4) restrict hNIS expression in prostatic tissue under transcriptional regulation of prostate-specific promoter.

14. SUBJECT TERMS	15. NUMBER OF PAGES
Prostate cancer, sodium iodide symporter, gene transfer, radioiodine	31
	16. PRICE CODE

17. SECURITY CLASSIFICATION OF REPORT	18. SECURITY CLASSIFICATION OF THIS PAGE	19. SECURITY CLASSIFICATION OF ABSTRACT	20. LIMITATION OF ABSTRACT
Unclassified	Unclassified	Unclassified	Unlimited

Table of Contents

INTRODUCTION

The sodium iodide symporter (NIS) mediates iodide uptake in thyroid follicular cells and provides a mechanism for effective radioiodide treatment of residual, recurrent, and metastatic thyroid cancers. The objective of the proposed research is to test the hypothesis that expression of exogenous hNIS in prostatic tissue will enable radioiodide to localize and ablate residual prostate cancer following prostatectomy, such that recurrence and metastasis of the disease can be prevented. The specific aims of this project are to: (1) confirm metastatic progression to distant lymph nodes and lungs following subcutaneous inoculation of rats with MATLyLu prostatic adenocarcinoma cells expressing hNIS; (2) investigate whether radioiodide therapy will prevent metastases and/or prolong survival in rats bearing subcutaneous MATLyLu tumors that express hNIS; (3) determine the expression level of hNIS required to elicit selective radioiodide-mediated killing of MATLyLu-hNIS prostatic adenocarcinoma cells *in vivo*; and, (4) restrict hNIS expression in prostatic tissue under transcriptional regulation of prostate-specific promoter.

BODY

Task 1. Confirm metastatic progression to distant lymph nodes and lungs following subcutaneous inoculation of rats with MATLyLu prostatic adenocarcinoma cells expressing hNIS ***<u>(completed in Year 1 with one published paper)</u>***

KMD La Perle, D Shen, TLF Buckwalter, B Williams, A Haynam, G Hinkle, R Pozderac, CC Capen, and SM **Jhiang** (2002) "*In Vivo* Expression and Function of the Sodium Iodide Symporter Following Gene Transfer in the MATLyLu Rat Model of Metastatic Prostate Cancer", *The Prostate*, **50**: 170-178.

Task 2. Investigate whether radioiodide therapy will prevent metastases and/or prolong survival in rats bearing subcutaneous MATLyLu tumors that express hNIS (Months 12-24, ***completed with 2 published papers***)

KMD La Perle, EAG Blomme, CC Capen, and SM **Jhiang** (2003) "Effect of Exogenous Human Sodium/Iodide Symporter Expression on Growth of MatLyLu Cells", *Thyroid* **13:**133-140

DHY Shen, DK Marsee, J Schaap, W Yang, J-Y Cho, G Hinkle, HN Nagaraja, RT Kloos, RF Barth, and SM **Jhiang** (2004) "Effects of dose, intervention time, and radionuclide on sodium iodide symporter (NIS) targeted radionuclide therapy", *Gene Therapy* **11:** 161-169.

Task 3. Determine the expression level of hNIS required to elicit selective radioiodide-mediated killing of MatLyLu-hNIS prostatic adenocarcinoma cells *in vivo* (not completed, modified study with 1 published paper)

Appendix 1: Knostman KA, Cho JY, Ryu KY, Lin X, McCubrey JA, Hla T, Liu CH, Di Carlo E, Keri R, Zhang M, Hwang DY, Kisseberth WC, Capen CC, **Jhiang** SM (2004) "Signaling through 3',5'-cyclic adenosine monophosphate and phosphoinositide-3 kinase induces sodium/iodide symporter expression in breast cancer", *J Clin Endocrinol Metab.* **89**:5196-203.

We hypothesize that radioiodide uptake *in vivo* correlates with NIS expression levels within a certain range. Unfortunately, we failed to acquire doxycycline-inducible prostate cancer cell lines despite several attempts. We then choose to study breast cancer cells which have hormone inducible endogenous NIS. We aim to identify the factors that could modulate NIS expression levels in breast cancer cell line, and then determine the expression level of NIS required eliciting selective radioiodide-mediated killing. Our studies showed that cAMP and PI3K signaling pathways are associated with increased NIS expression in mouse mammary gland tumors (appendix 1).

Task 4. Restrict hNIS expression in prostatic tissue under transcriptional regulation of prostate-specific promoters (not completed, modified studies with 3 published papers)

DK Marsee, DHY Shen, LR MacDonald, DD Vadysirisack, X Lin, G Hinkle, RT Kloos, SM Jhiang (2004) "Imaging of Pulmonary Tumors Following NIS Gene Transfer Using Single Photon Emission Computed Tomography", *Cancer Gene Therapy* **11**:121-127.

Appendix 2: Lin X, Ryu KY, **Jhiang** SM (2004) "Cloning of the 5'-flanking region of mouse sodium/iodide symporter and identification of a thyroid-specific and TSH-responsive enhancer", *Thyroid* **14**:19-27.

Appendix 3: Lin X, Fischer AH, Ryu KY, Cho JY, Sferra TJ, Kloos RT, Mazzaferri EL, **Jhiang** SM (2004) "Application of the Cre/loxP system to enhance thyroid-targeted expression of sodium/iodide symporter", *J Clin Endocrinol Metab.* **89**:2344-50.

In order to better investigate the transcriptional regulation of the NIS gene, we cloned and characterized the 3.2 kb 5'-flanking region of the mouse NIS (mNIS) gene. We identified the minimal promoter region as well as a thyroid-specific and TSH-responsive enhancer (Appendix 1). Since all advanced cancer are most likely to loss the ability to express tissue specific proteins. We investigated the application of the Cre/loxP system to enhance thyroid-targeted hNIS expression driven by thyroglobulin (Tg) promoter. We showed that for tumors with weak tissue specific promoter activity, Cre/loxp system induced higher hNIS expression (appendix 3)

KEY RESEARCH ACCOMPLISHMENTS

- Show that signaling through 3',5'-cyclic adenosine monophosphate and phosphoinositide-3 kinase induces sodium/iodide symporter expression in breast cancer
- Cloned and characterized the 5'-flanking region of the mouse NIS gene
- Demonstrate that Cre/loxp system is effective in tumors with weak tissue specific promoter activity

REPORTABLE OUTCOMES

Manuscript 1: Knostman KA, Cho JY, Ryu KY, Lin X, McCubrey JA, Hla T, Liu CH, Di Carlo E, Keri R, Zhang M, Hwang DY, Kisseberth WC, Capen CC, **Jhiang** SM (2004) "Signaling through 3',5'-cyclic adenosine monophosphate and phosphoinositide-3 kinase induces sodium/iodide symporter expression in breast cancer", *J Clin Endocrinol Metab*. **89**:5196-203.

Manuscript 2: Lin X, Ryu KY, **Jhiang** SM (2004) "Cloning of the 5'-flanking region of mouse sodium/iodide symporter and identification of a thyroid-specific and TSH-responsive enhancer", *Thyroid* **14**:19-27.

Manuscript 3: Lin X, Fischer AH, Ryu KY, Cho JY, Sferra TJ, Kloos RT, Mazzaferri EL, **Jhiang** SM (2004) "Application of the Cre/loxP system to enhance thyroid-targeted expression of sodium/iodide symporter", *J Clin Endocrinol Metab*. **89**:2344-50.

CONCLUSIONS

- NIS-mediated radionuclide imaging and therapy can be applied to prostate cancer provided that gene delivery efficacy and specificity could be achieved.
- NIS can serve as an imaging reporter gene to optimize vector delivery for prostate cancer gene therapy.

APPENDICES

Three manuscripts are appended.

0021-972X/04/$15.00/0
Printed in U.S.A.

The Journal of Clinical Endocrinology & Metabolism 89(10):5196–5203

doi: 10.1210/jc.2004-0907

Signaling through 3′,5′-Cyclic Adenosine Monophosphate and Phosphoinositide-3 Kinase Induces Sodium/Iodide Symporter Expression in Breast Cancer

KATHERINE A. B. KNOSTMAN, JE-YOEL CHO, KWON-YUL RYU, XIAOQIN LIN, JAMES A. McCUBREY, TIMOTHY HLA, CATHERINE H. LIU, EMMA DI CARLO, RUTH KERI, MING ZHANG, DAE Y. HWANG, WILLIAM C. KISSEBERTH, CHARLES C. CAPEN, AND SISSY M. JHIANG

Departments of Veterinary Biosciences (K.A.B.K., C.C.C.), Veterinary Clinical Sciences (W.C.K.), and Physiology and Cell Biology (S.M.J.), The Ohio State University, Columbus, Ohio 43210; Department of Biochemistry (J.-Y.C.), School of Dentistry, Kyungpook National University, Daegu 700-42, Republic of Korea; Department of Biological Sciences (K.-Y.R.), Stanford University, Stanford, California 94305; Department of Biological Chemistry (X.L.), University of California, Irvine, Irvine, California 92697; Department of Microbiology and Immunology (J.A.M.), East Carolina University School of Medicine, Greenville, North Carolina 27858; Center for Vascular Biology (T.H.), University of Connecticut Health Center, Farmington, Connecticut 06030; Department of Molecular Genetics, Microbiology, and Immunology (C.H.L.), University of Medicine and Dentistry of New Jersey, Piscataway, New Jersey 08854; Department of Oncology and Neurosciences (E.D.C.), "G. d'Annunzio" University, 66100 Chieti, Italy; Department of Pharmacology (R.K.), Case School of Medicine, Case Western Reserve University, Cleveland, Ohio 44106; Department of Molecular and Cellular Biology (M.Z.), Baylor College of Medicine, Houston, Texas 77030; and Division of Laboratory Animal Resources (D.Y.H.), National Institute of Toxicological Research, Korea Food and Drug Administration, Seoul 122-704, Republic of Korea

The sodium/iodide symporter (NIS) is a membrane transport glycoprotein normally expressed in the thyroid gland and lactating mammary gland. NIS is a target for radioiodide imaging and therapeutic ablation of thyroid carcinomas and has the potential for similar use in breast cancer treatment. To facilitate NIS-mediated radionuclide therapy, it is necessary to identify signaling pathways that lead to increased NIS expression and function in breast cancer. We examined NIS expression in mammary tumors of 14 genetically engineered mouse models to identify genetic manipulations associated with NIS induction. The cAMP and phosphoinositide-3 kinase (PI3K) signaling pathways are associated with NIS up-regulation. We showed that activation of PI3K alone is sufficient to increase NIS expression and radioiodide uptake in MCF-7 human breast cancer cells, whereas cAMP stimulation increases NIS promoter activity and NIS mRNA levels but is not sufficient to increase radioiodide uptake. This study is the first to demonstrate that NIS expression is induced by cAMP and/or PI3K in breast cancer both *in vivo* and *in vitro*. (*J Clin Endocrinol Metab* 89: 5196–5203, 2004)

BREAST CANCER IS one of the leading causes of cancer in women in the United States, with more than 181,000 newly diagnosed cases and in excess of 44,000 cancer-related deaths annually (1). Several specific genetic mutations and environmental factors leading to an increased risk of breast cancer have been elucidated in recent years. Conventional treatment modalities for breast cancer include radical mastectomy, lumpectomy with radiotherapy, systemic hormone modulating therapy (tamoxifen and raloxifene), and chemotherapy (1, 2). Diagnosis is currently made at an earlier stage of the disease due to increased use of mammography and routine clinical examination, which together have decreased mortality by 25–30% in women over 50 yr old. However, monitoring recurrence and metastases by frequent physical examination in breast cancer patients has not been successful in changing the clinical course, and most women with metastatic carcinoma will eventually die from the disease. Therefore, detection and treatment of recurrent and metastatic breast cancer is of high clinical importance.

The sodium/iodide symporter (NIS) is a transmembrane glycoprotein most commonly studied in the context of the thyroid gland, in which it mediates active transport of iodide (I^-) from the systemic circulation into thyroid follicular cells. NIS forms the basis of radioiodide treatment for thyroid cancer by facilitating targeted radioiodide uptake and subsequent destruction of residual and/or metastatic neoplastic cells after thyroidectomy (3, 4). Additionally, NIS-expressing thyroid tumors can be imaged using nuclear scintigraphy, improving detection of residual, recurrent, or metastatic lesions.

In addition to the thyroid gland, the salivary glands, gastric mucosa, lacrimal system, placenta, and lactating mammary gland express NIS and thus have the capacity to actively accumulate iodide (5). Our unpublished data as well

Abbreviations: 8-Br-cAMP, 8-Bromoadenosine-cAMP; ChT, cholera toxin; Cox, cyclooxygenase; ddH_2O, double-distilled water; FBS, fetal bovine serum; GAPDH, glyceraldehyde-3-phosphate dehydrogenase; GEM, genetically engineered mice; hCG, human chorionic gonadotropin; H&E, hematoxylin and eosin; IBMX, 3-isobutyl-1-methylxanthine; MMTV, mouse mammary tumor virus; NIS, sodium/iodide symporter; PGE2, prostaglandin E2; PI3K, phosphoinositide-3 kinase; PyMT, polyoma virus middle T antigen; SV40, Simian virus 40; TBS, Tris-buffered saline; tRA, *trans*-retinoic acid.

JCEM is published monthly by The Endocrine Society (http://www.endo-society.org), the foremost professional society serving the endocrine community.

as that of others (5, 6) have demonstrated NIS protein in the majority of human breast cancers using immunohistochemistry. The fact that NIS is up-regulated in lactating mammary epithelial cells and that increased NIS expression is detected in many human breast tumors raises the potential for developing NIS-mediated radionuclide therapy as a safe and effective treatment for breast cancer.

The use of genetically engineered mice (GEM) has greatly increased understanding of mammary tumorigenesis, offering a convenient system for studying the interaction of specific genetic manipulations with external factors. Tumors from Her-2/neu and v-Ha-ras transgenic mice have been reported to express NIS and could be imaged using scintigraphy (5). Recently Kogai *et al.* (7) demonstrated *trans*-retinoic acid (tRA)-induced NIS mRNA expression and ^{125}I uptake in mammary tumors from polyoma virus middle T antigen mice.

The objectives of the current study included evaluating NIS expression in mammary tumors of 14 GEM models to identify genetic manipulations that lead to increased NIS expression *in vivo* and investigating the role of associated signaling pathways in NIS induction *in vitro* using MCF-7 human mammary carcinoma cells. Based on the four transgenes associated with NIS induction, we identified that signaling pathways mediated by cAMP and phosphoinositide-3 kinase (PI3K) are important in NIS up-regulation. We further demonstrated that activation of PI3K alone is sufficient to increase NIS expression and radioiodide uptake in MCF-7 human breast cancer cells, whereas cAMP stimulation increases NIS promoter activity and NIS mRNA levels but is not sufficient to increase radioiodide uptake.

Materials and Methods

Transgenic mice

We requested unstained tissue sections from 14 GEM models of breast cancer. Table 1 summarizes the models investigated for NIS expression using immunohistochemistry and references for each model. Investigators who made tissue samples available are indicated in *Acknowledgments* at the conclusion of this manuscript. The four transgenic mouse models with high NIS expression are discussed in further details as follows.

Tissue sections from Ubi-human chorionic gonadotropin (hCG)β transgenic mice were obtained from Dr. Ilpo Huhtaniemi (University of Turku, Turku, Finland). The transgene, which was introduced into an FVB/N background, consisted of a 579-bp cDNA segment of the hCGβ gene driven by a 1.2-kb ubiquitin C promoter (8). Transgenic female Ubi-hCGβ mice were obese, underwent precocious puberty, and had abnormal estrous cycles leading to infertility. Females had abnormally high serum estradiol levels until 2 months of age, at which time it returned to normal. Serum progesterone, testosterone, and prolactin levels gradually increased from the age of 4–6 months until 12 months. Pituitary glands in female Ubi-hCGβ transgenic mice developed lactotrope hyperplasia and adenomas by the age of 10–12 months. Mammary glands had marked lobuloalveolar hyperplasia by age 6 months, similar in phenotype to pregnancy, which progressed to mammary tumors by age 12 months in 91% of transgenic females. The histologic appearance of mammary adenocarcinomas varied from well-differentiated papillary carcinomas with abundant intraluminal secretions to poorly differentiated solid variants. Tumors had high mitotic indices and were highly invasive, with metastases to liver, lung, spleen, uterus, and adrenal glands occurring in nearly half of all cases. Ovariectomy at 6 wk of age completely prevented glandular hyperplasia and neoplasia.

Tissue sections from mouse mammary tumor virus (MMTV)-cyclooxygenase (Cox)-2 mice were obtained from Dr. Timothy Hla (University of Connecticut Health Center, Farmington, CT). The transgene, consisting of the human Cox-2 gene open reading frame driven by the promoter of the MMTV, was injected into a CD1 background strain (9). High Cox-2 expression was detected in mammary gland tissue, particularly during lactation, and transgenic females exhibited premature mammary development. Involution was delayed from the normal 1–2 d until 7 d post weaning by virtue of decreased apoptosis of mammary epithelial cells. Multiparous females developed frequent hyperplastic alveolar nodules, and approximately 85% developed mammary adenocarcinomas. Histologically, tumors consisted of moderately to well-differentiated ductal and lobuloalveolar adenocarcinomas with frequent squamous metaplasia, scirrhous reaction, and neovascularization. Metastases to lymph nodes occurred in many MMTV-Cox-2 females.

Mammary tissue sections from MMTV-polyoma virus middle T antigen (PyMT) transgenic mice were obtained from Dr. Donna Kusewitt

TABLE 1. Immunohistochemical detection of NIS expression in mouse models of breast cancer

Model	Ref.	n	No. positive (%)	% Cells positive	Intensity	Subcellular localization
Ubi-hCGβ	8	5	5 (100)	100	4+	PM
MMTV-neu	12, 13	9	8 (100)	100	4+	PM, C
MMTV-PyMT	10	3	3 (100)	100	4+	PM
MMTV-Cox-2	9	2	2 (100)	100	3+	PM, C
α-LH/CTP[a]	38	4	4 (100)	100	1–2+	PM, C
WAP-p53^{R172H} + DMBA + pituitary isograft[b]	39	4	4 (100)	100	1+	C
C3(1)-TAg[c]	40	5	2 (40)	50	1+	PM, C
p53$^{-/-}$ mammary explants + DMBA + pituitary isograft[d]	41	3	3 (100)	100	1+	C
WAP-*des*-IGF-1[e]	42	2	0 (0)	0	0	N/A
WAP-p53^{R172H} × WAP-*des*-IGF-1[f]	42	4	0 (0)	0	0	N/A
MMTV-HPV16E6/β-casein[g]	43	1	0 (0)	0	0	N/A
WAP-Tag × WAP-maspin[h]	44	2	0 (0)	0	0	N/A
MMTV-c-myc × MMTV-v-Ha-ras[i]	45	3	0 (0)	0	0	N/A
DMBA + pituitary isograft only[j]	41	5	0 (0)	0	0	N/A

PM, Plasma membrane; C, cytoplasm; N/A, not applicable.
[a] Glycoprotein α-subunit promoter driving LH/C-terminal peptide fusion gene.
[b] Whey acidic protein promoter driving p53 R172H mutant gene with DMBA carcinogen and implantation of pituitary isograft.
[c] Prostate steroid binding protein C3 (1) promoter driving SV40 large T antigen gene.
[d] p53 null mammary explants implanted in wild-type mice treated with DMBA and pituitary isograft.
[e] Whey acidic protein promoter driving IGF gene.
[f] Bitransgenic mice expressing mutant p53 and IGF-I.
[g] Mouse mammary tumor virus promoter driving human papillomavirus 16E6 subunit/β-casein fusion gene.
[h] Bitransgenic mice expressing SV40 large T antigen and maspin tumor suppressor gene.
[i] Bitransgenic mice expressing c-myc and v-Ha-ras oncogenes.
[j] Wild-type mice treated with DMBA and pituitary isografts.

(Ohio State University, Columbus, OH). The transgene consisted of the *PyMT* gene open reading frame driven by the promoter of the MMTV. Mammary tumorigenesis was evident by the age of 5 wk, although very early lesions of atypical ductular hyperplasia sometimes preceded neoplasia. Histologically, tumors were solid to cystic, multicentric, often poorly differentiated, invasive, and widely metastatic (10, 11).

Tissue sections from MMTV-neu transgenic mice were acquired from Dr. Emma Di Carlo (G. d'Annunzio University, Chieti, Italy), and tissue sections from MMTV-c-neu transgenic mice were obtained from Dr. William Kisseberth (The Ohio State University, Columbus, OH). MMTV-neu mice from G. d'Annunzio University were created by insertion of the transgene, consisting of the MMTV promoter driving expression of the activated rat *neu* oncogene, into a BALB/c background strain (12). Widespread atypical hyperplasia of small lobular ducts and lobules was already evident in mammary tissue at the third week of age, progressing to lobular carcinoma *in situ* by the 10th to 11th week and finally to multiple invasive carcinomas at approximately 20 wk of age, which involved all 10 mammary glands by the age of 33 wk. MMTV-c-neu mice from The Ohio State University were created by insertion of the transgene, consisting of the MMTV promoter driving expression of the unactivated rat *c-neu* protooncogene, into an FVB/N background strain (13). These mice developed focal mammary carcinomas between the ages of 4 and 11 months of age with development of lung metastases in approximately 40–75% of mice (variation was present among different transgenic mouse lines).

Immunohistochemistry

Paraffin-embedded formalin- or paraformaldehyde-fixed murine mammary tissue was sectioned to 5 μm thickness and affixed to glass slides. Deparaffinization and rehydration were performed as follows: slides were submerged in 100% xylene for three repetitions of 5 min each, followed by submersion into 100% ethanol for two repetitions of 2 min each, 95% ethanol for 2 min, and 70% ethanol for two repetitions of 2 min each. Next, slides were gently washed in double-distilled water (ddH_2O) for 2 min. Endogenous peroxidase activity was blocked by soaking slides in 3% hydrogen peroxide in methanol for 15 min. After gently washing slides in ddH_2O, antigen retrieval was performed by dipping slides in steaming ddH_2O and placing them into steaming citric acid buffer (citrate, sodium citrate, and ddH_2O) for 30 min. After antigen retrieval, slides were cooled by soaking in lukewarm ddH_2O and then rinsed in Tris-buffered saline [TBS; 3% 5 N NaCl, 1% 1 M Tris (pH 8.0), and 96% ddH_2O] with gentle agitation. Next, slides were placed in a humidified chamber and blocked at 4 C overnight using 2% BSA in TBS. The following day, BSA was removed by aspiration and rabbit antirat NIS primary antibody, which cross-labels mouse NIS (PA716, a kind gift from Dr. Bernard Rousset, Institut National de la Santé et de la Recherche Médicale, Lyon, France; diluted 1:1000 in 1% BSA) was immediately applied to slides, which were then incubated in a humidified chamber at room temperature for 1 h. Negative control slides were incubated with 1% BSA alone. After 1 h, slides were washed with TBS to remove residual primary antibody. Horseradish peroxidase-conjugated goat antirabbit secondary antibody (Bio-Rad Laboratories, Hercules, CA) was diluted 1:250 in 1% BSA and applied to slides for 20 min incubation in a humidified chamber at room temperature. Slides were rinsed in TBS to remove residual secondary antibody. Antigen-antibody complexes were detected by incubation of tissue sections with chromagen DAB (Dako, Carpinteria, CA) for 5 min in a dark chamber at room temperature. Slides were rinsed in ddH_2O three times with gentle agitation, counterstained with Gill's hematoxylin (Fisher Scientific, Pittsburgh, PA) for 30 sec, dipped in running lukewarm tap water, placed in clarifier for 1 min, rinsed a second time in running lukewarm tap water, and dipped in a bluing agent (1% NH_4OH). Dehydration was performed by dipping slides in a progression of 70% ethanol, 95% ethanol, 100% ethanol, and 100% xylene. Slides were then air dried and coverslipped.

Cell culture

MCF-7 cells were maintained in medium consisting of equal parts DMEM and Ham's F12, 10% fetal bovine serum (FBS), and 1% penicillin/streptomycin (Invitrogen, Carlsbad, CA) and kept in a 37 C incubator with 5% CO_2. When applicable, cells were treated with 2, 5, or 10 IU/ml hCG (Dr. A. F. Parlow, National Hormone and Peptide Program, Torrance, CA) or 1 μM prostaglandin E2 (PGE2; Sigma, St. Louis, MO) for 24 or 48 h before radioiodide uptake assay. In experiments requiring treatment with tRA, 3-isobutyl-1-methylxanthine (IBMX), 8-bromoadenosine-cAMP (8-Br-cAMP), or cholera toxin (ChT; all from Sigma), charcoal-stripped culture medium was used (equal parts DMEM and Ham's F12, 5% charcoal-stripped FBS, and 1% penicillin/streptomycin). When culturing MCF-7 cells treated with PGE2 or MCF-7 stable clones expressing pBpuro, v-Ha-ras, or PI3K, cells were maintained in 89% RPMI 1640 with glutamine (Invitrogen), 10% FBS, and 1% penicillin/streptomycin. PC Cl 3 rat thyroid cells were cultured in 91% Coon's modified F-12 medium with 5% calf serum, 1% 200 mM glutamine, 1% 1 M sodium bicarbonate, 1% penicillin/streptomycin, and 1% of a six-hormone mixture (1 nM TSH, 10 μg/ml insulin, 10 ng/ml somatostatin, 5 μg/ml transferrin, 10 nM hydrocortisone, and 10 ng/ml glycyl-L-histidyl-L-lysine acetate; all from Sigma).

DNA constructs

NIS promoter-luciferase reporter gene constructs, 144-bp hNISp and 2.9-kb hNISp, were engineered using the PGL_2B vector as described by Ryu *et al.* (14). Recombinant retroviruses encoding v-Ha-ras, PI3K p110 active, and empty vector pBpuro were obtained from Dr. Michael Weber (University of Virginia, Charlottesville, VA), Dr. Julian Downward (Imperial College Research Fund, London, UK), and Dr. Martin McMahon (University of California, San Francisco). MCF-7 stable clones expressing pLXSN/v-Ha-ras, pLXSN/PI3K p110 CAAX (constitutively active), and empty vector pBpuro were generated by retroviral infection of MCF-7 cells in the laboratory of Dr. James McCubrey (East Carolina University, Greenville, NC) as described by Davis *et al.* (15).

Luciferase assay

Approximately 1× 10^5 MCF-7 cells were seeded in each well of a 6-well plate. After 24 h, cells were transfected with human NIS promoters (2.9-kb hNISp, 144-bp hNISp, or PGL_2C control vectors) using Lipofectamine (Invitrogen). The culture medium was then changed to 5% charcoal-stripped medium, and cells were treated with IBMX (10 μM) and ChT (10 ng/ml) for 24 h. Cells were harvested, and luciferase assays were performed using a luciferase assay kit (Promega, Madison, WI) and luminometer (Lumat; PerkinElmer, Boston, MA). As a positive control, the PGL_2-C control vector with the Simian virus 40 (SV40) promoter showed high basal activities but no further activation by IBMX+ChT treatment. Normalization of transfection efficiency was determined by cotransfecting cells with the plasmid pCH110 (SV40-LacZ). Within each treatment group, luciferase activity was normalized to β-galactosidase activity.

Quantitative real-time PCR

Quantitative real-time PCR assay was performed as described by our laboratory (16). Briefly, 5× 10^5 MCF-7 cells were seeded in normal culture medium in 35-mm plates. Medium was changed to charcoal-stripped MCF-7 medium 1 d before treatment with 8-Br-cAMP or IBMX and ChT. RNA was isolated 24 h after treatment using TRIzol reagent (Invitrogen). One microgram of RNA was used for the reverse transcription reaction. Two microliters of cDNA template were used for quantitative real-time PCR, which used the human NIS dual-probe quantification method. For glyceraldehyde-3-phosphate dehydrogenase (GAPDH) normalization, 236 bp human GAPDH was amplified by PCR using two primers: GAPDH-F1 (TTC ACC ACC ATG GAG AAG GC) and GAPDH-R1 (GGC ATG GAC TGT GGT CAT GA). The amplified DNA fragment was cloned into the TA cloning vector, maxiprepped (Qiagen, Valencia, CA) and used as the standard for SYBR Green I quantitative real-time PCR. The data were presented as a fold increase over control after NIS mRNA levels were normalized with GAPDH mRNA levels.

Radioiodide uptake assay

Radioiodide uptake assay was performed essentially as in La Perle *et al.* (17). Twelve-well plates were seeded with 5× 10^4 MCF-7 cells per well. Assays were performed in triplicate. MCF-7 cells were treated with hCG or PGE2 for 24 or 48 h when applicable, after which time the cells were incubated with 2 μCi/well of ^{125}I in NaI for 30 min at 37 C. Cells were rapidly washed twice with 1 ml cold Hanks' balanced salt solution and incubated in 1 ml 95% ethanol at room temperature for 20 min to release intracellular ^{125}I. The supernatant was counted in a γ-radiation counter. Counts per minute were normalized to cell number (1×10^5). MCF-7 cells treated with tRA were used as a positive control (18).

Statistical analysis

Statistical analysis consisted of Student's *t* test and was performed using GraphPad software (GraphPad Inc., San Diego, CA). Each experimental group was compared with its respective control group.

Results

Of the 14 GEM models evaluated (Table 1), mammary tumors from transgenic mice expressing the oncogenes *PyMT* and *neu* (both activated and unactivated forms) were strongly positive for NIS using immunohistochemical staining, as were transgenic mice expressing the hCGβ subunit and the enzyme Cox-2 in the mammary gland (Fig. 1, A–K). NIS staining was primarily plasma membrane localized in all four models, although light cytoplasmic staining was present in Cox-2 and neu tumors. Lesions of lobular hyperplasia were available from activated neu and hCGβ mice. All of these lesions had strong plasma membrane staining for NIS (Fig. 1, G and J). Additionally, two samples from histologically normal juvenile c-neu mouse mammary glands were found to be strongly positive for NIS (Fig. 1F), whereas nonlactating mammary glands of nontransgenic mice did not express NIS (data not shown).

Upon examination of the available scientific literature concerning signal transduction pathways activated by the four transgenes (8–13, 19–22), we identified two signaling pathways of interest for further *in vitro* study. We hypothesize

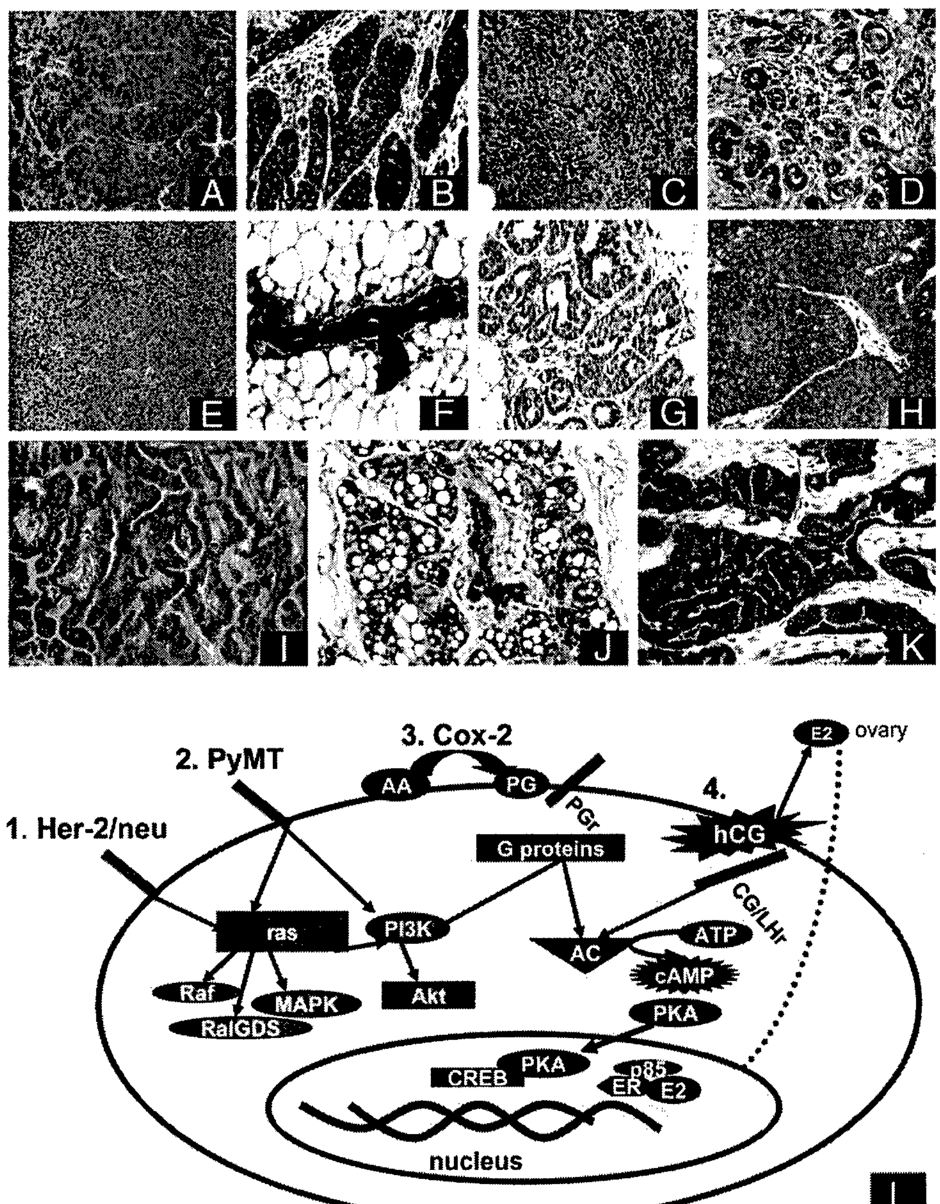

FIG. 1. A–K, Histology and immunohistochemical staining for NIS expression in mouse models of breast cancer (magnification, ×400). A, Carcinoma from MMTV-PyMT mouse mammary gland [hematoxylin and eosin (H&E)]. B, Strongly positive immunohistochemical staining for NIS in a PyMT mouse mammary tumor. C, Adenocarcinoma with marked lymphocytic infiltration from a MMTV-Cox-2 mouse mammary gland (H&E). D, Strongly positive immunohistochemical staining for NIS in a Cox-2 mouse mammary adenocarcinoma. E, Carcinoma from a MMTV-neu mouse mammary gland (H&E). F, Strongly positive immunohistochemical staining for NIS in a normal mammary duct from a juvenile MMTV-c-neu mouse. G, Strongly positive immunohistochemical staining for NIS in a lesion of lobular hyperplasia from a MMTV-neu mouse mammary gland. H, Strongly positive immunohistochemical staining for NIS in a MMTV-neu mammary carcinoma. I, Ductular carcinoma from a Ubi-hCGβ mouse mammary gland (H&E). J, Strongly positive immunohistochemical staining for NIS in a lesion of ductular hyperplasia from a Ubi-hCGβ mouse mammary gland. K, Strongly positive immunohistochemical staining for NIS in a Ubi-hCGβ mammary carcinoma. L; *lower panel*) Signaling pathways up-regulated in the four above transgenic mouse models with potential roles in NIS induction. Her-2/neu and PyMT oncogenes use Ras and PI3K signal transduction pathways. Prostaglandins induced by the Cox-2 enzyme activate adenylyl cyclase and increase cAMP levels but also interact with PI3K. hCG induces adenylyl cyclase activity, increasing intracellular cAMP but also stimulates estradiol (E2) release from the ovaries *in vivo*.

that cAMP elevation in hCGβ and Cox-2 mice and PI3K activation in *PyMT* and *Her-2/neu* mice are responsible for NIS induction in the corresponding mammary glands and mammary tumors (Fig. 1L, *bottom panel*).

Using the LH/CG receptor-positive MCF-7 human mammary carcinoma cell line, we showed that hCG treatment induces radioiodide uptake, an indication of NIS function (Fig. 2). We also showed that PGE2 treatment induces radioiodide uptake (Fig. 3). Cox-2 is critical in catalyzing the conversion of arachidonic acid to prostaglandins, such as PGE2. Because cAMP signaling plays an important role in hCG signaling and is induced by PGE2 treatment of MCF-7 cells (23), we further investigated the importance of cAMP in NIS induction *in vitro*. We showed that increasing intracellular cAMP levels using the phosphodiesterase inhibitor IBMX in combination with the adenylyl cyclase inducer ChT, or alternatively by administration of 8-Br-cAMP, markedly stimulated NIS mRNA expression in MCF-7 cells (Figs. 4 and 5). Interestingly, administration of high doses of IBMX and ChT resulted in less induction of NIS expression than did the lower doses. To determine whether cAMP has a direct effect on the NIS promoter, MCF-7 cells were transiently transfected with NIS promoter-reporter gene constructs consisting of either a 144-bp minimal promoter or a 2.9-kb 5′ flanking region driving expression of the luciferase reporter gene. In cells treated with IBMX and ChT, activities of both the minimal promoter and the 2.9-kb NIS promoter were increased more than 10-fold (Fig. 6), indicating that a cAMP response element is present in these promoter regions.

The importance of signal transduction through PI3K was investigated using MCF-7/PI3K stable clones. Stable clones expressing the constitutively active PI3K p110 catalytic subunit had greater than 4-fold increase in radioiodide uptake, compared with empty vector-expressing cells (Fig. 7). Stable clones expressing v-Ha-ras, one upstream mediator of PI3K activity, had slightly increased iodide uptake, compared with negative control cells. These findings reveal that PI3K overexpression is sufficient to induce NIS function in MCF-7 breast cancer cells.

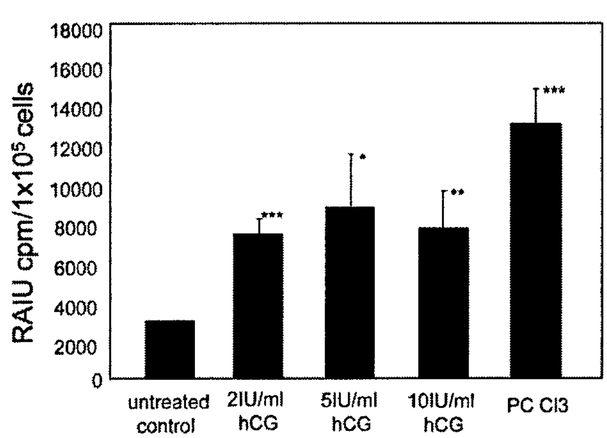

FIG. 2. Treatment of MCF-7 cells with hCG induces radioiodide uptake. MCF-7 cells in medium were incubated with 2, 5, or 10 IU/ml recombinant hCG for 48 h, after which radioiodide (^{125}I) uptake assay was performed in triplicate. Treatment with 5 IU/ml hCG resulted in a 4-fold increase in uptake. PC Cl 3 rat thyroid cells were used as a positive control. *, $P < 0.05$; **, $P < 0.01$; ***, $P < 0.001$.

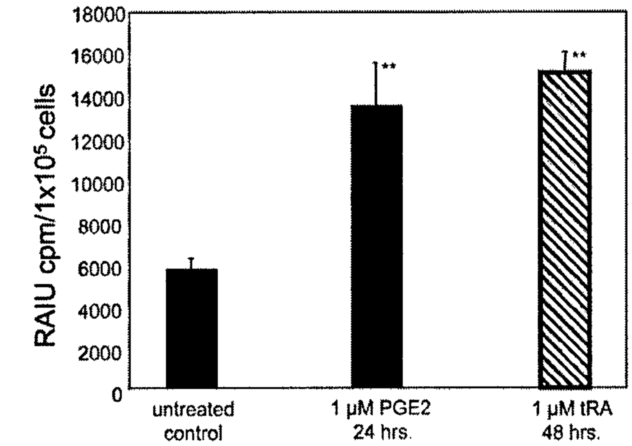

FIG. 3. Treatment of MCF-7 cells with PGE2 induces radioiodide uptake. MCF-7 cells were incubated with 1 μM PGE2 for 24 or 48 h, after which radioiodide (^{125}I) uptake assay was performed. Treatment with PGE2 for 24 h resulted in a 2.5-fold increase in uptake. MCF-7 cells treated with tRA were used as a positive control. **, $P < 0.01$.

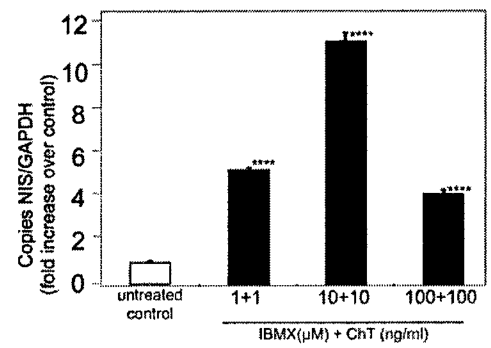

FIG. 4. Treatment of MCF-7 cells with IBMX and ChT induces NIS mRNA expression. MCF-7 cells were incubated with the phosphodiesterase inhibitor IBMX and the adenylyl cyclase stimulator ChT alone or in combination for 24 h, after which time quantitative real-time PCR for NIS expression was performed. NIS expression was normalized to GAPDH. Treatment of cells with 10 μM IBMX and 10 ng/ml ChT resulted in an 11-fold induction of NIS expression. ****, $P < 0.0001$.

Discussion

This study is the first to demonstrate the importance of cAMP and PI3K signaling in NIS regulation in the context of the mammary gland. We showed that activation of PI3K alone is sufficient to increase NIS expression and radioiodide uptake in MCF-7 human breast cancer cells, whereas cAMP stimulation increases NIS promoter activity and NIS mRNA levels but is not sufficient to increase radioiodide uptake (see Ref. 18 and our unpublished data).

We found that MMTV-Cox-2 and Ubi-hCGβ transgenic mice had high levels of NIS expression in their mammary tumors and that treatment of MCF-7 breast cancer cells with PGE2 or hCG stimulated radioiodide uptake. The signaling cascades downstream of PGE2 and hCG are similar, involving G protein-coupled receptors, cAMP up-regulation, and protein kinase A activation. In Cox-2 transgenic mice, up-regulation of the PGE2 receptors, EP2 and EP4, has been detected in mammary tumors, confirming that PGE2 signaling is activated in this system (24). Planchon *et al.* (23) showed

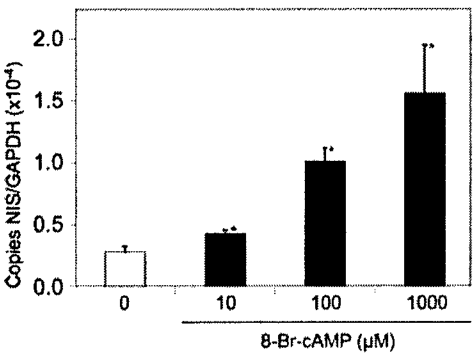

FIG. 5. Treatment of MCF-7 cells with 8-Br-cAMP induces NIS mRNA expression in a dose-dependent manner. MCF-7 cells were treated with 8-Br-cAMP for 24 h, after which time quantitative real-time PCR for NIS expression was performed. NIS expression was normalized to GAPDH. Administration of 1000 μM 8-Br-cAMP resulted in a greater than 5-fold increase in NIS mRNA transcripts. *, $P < 0.05$.

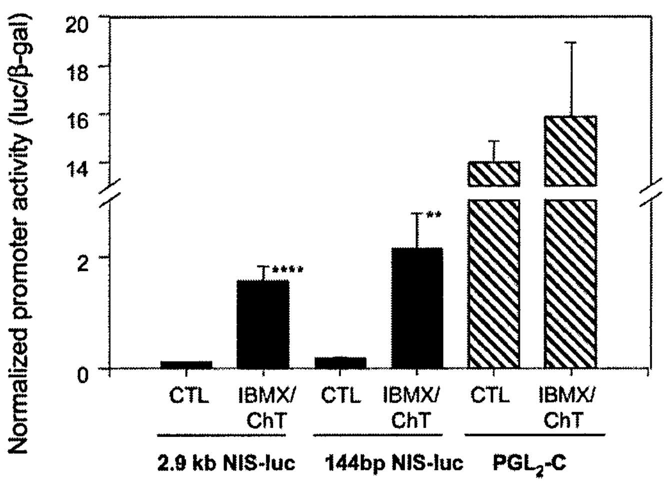

FIG. 6. Treatment of MCF-7 cells with IBMX and ChT stimulates activity of the NIS minimal promoter and 2.9-kb promoter. MCF-7 cells were transiently transfected with pGL$_2$B constructs containing either the 144-bp NIS minimal promoter or a 2.9-kb promoter-driving expression of the luciferase reporter gene. PGL$_2$-C, which contains an SV40 promoter, was used as a positive control. Cotransfection with a SV40-LacZ construct (pCH110) was performed for normalization of transfection efficiency. Immediately after the completion of transfection, cells were treated with 10 μM IBMX and 10 ng/ml ChT. After 24 h, luciferase assay was performed. Activity of the NIS minimal promoter and the 2.9-kb promoter were stimulated more than 10-fold by treatment with IBMX and ChT, indicating that cAMP-response elements are present in these regions. CTL, Untreated control. **, $P < 0.01$; **** $P < 0.0001$.

that treatment of MCF-7 cells with PGE2 induced cAMP levels by more than 10-fold over untreated controls. Treatment with hCG also increased NIS expression in JAr human choriocarcinoma cells via interaction with the LH/CG receptor (25) and in rat FRTL-5 thyroid cells via interaction with the TSH receptor (26).

We demonstrated that treatment of MCF-7 cells with compounds that increase intracellular cAMP levels (IBMX, ChT, and 8-Br-cAMP) led to a significant increase in NIS mRNA levels and NIS promoter activity (Figs. 4–6). Interestingly, treating MCF-7 cells with forskolin, an adenylyl cyclase activator, was not sufficient to increase radioiodide uptake (see Ref. 18 and our unpublished data). It is possible that, whereas increasing cAMP levels leads to increased NIS transcription, it does not result in sufficient protein levels or cell surface trafficking to have a significant effect on radioiodide uptake in MCF-7 cells. Thus, the effect of cAMP on NIS expression in MCF-7 cells is different from that in thyroid follicular cells. TSH up-regulates NIS expression and radioiodide uptake through interaction with TSH receptors in the plasma membrane, Gα-protein mediation, and an increase in cAMP (4, 14, 27), and NIS up-regulation can be fully reproduced through administration of cAMP agonists, such as forskolin. Thus, whereas the effects of hCG and PGE2 on NIS regulation the mammary gland context are similar to those of TSH in thyroid follicular cells, the pathways are not identical with respect to the effect of cAMP on radioiodide uptake.

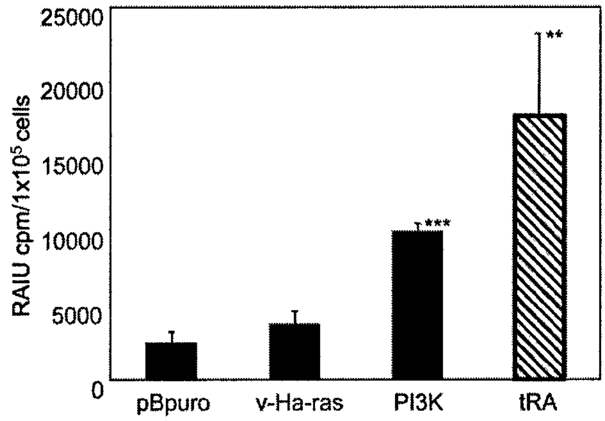

FIG. 7. MCF-7 cells stably expressing PI3K have increased radioiodide uptake. MCF-7 stable clones expressing empty pBpuro vector, v-Ha-ras, or constitutively active PI3K were assessed for radioiodide uptake ability. MCF-7/PI3K cells had 4-fold greater iodide uptake ability than did vector-only control cells. MCF-7/v-Ha-ras cells had 1.5-fold higher radioiodide uptake ability than did the vector-only cells, which was not statistically significant. MCF-7 cells treated with tRA were used as a positive control. **, $P < 0.01$; ***, $P < 0.001$.

Lactogenic hormones are critical in NIS regulation in the mammary gland (5, 16, 28), yet the signal transduction pathways stimulated by these hormones leading to increased NIS expression have not been characterized. In general, prolactin functions via activation of downstream signal transduction through MAPK and/or PI3K (29, 30), and oxytocin uses protein kinase C/phospholipase C and Ras/Raf/MAPK (31). Transient transfection of mutant rasV12S35, which preferentially interacts with the downstream effector Raf-1, abolished NIS expression in TSH-stimulated Wistar rat thyroid (WRT) cells (32, 33). The rasV12C40 mutant, which interacts primarily with PI3K, maintained NIS expression. Our finding of increased radioiodide uptake in MCF-7/PI3K stable clones demonstrates that overexpression of PI3K alone is sufficient to induce NIS function in MCF-7 cells. It is interesting to note that Lin *et al.* (11) discovered frequent induction of *neu* expression in PyMT mammary tumors, which was confirmed in our study (data not shown). Thus, NIS induction in the mammary tumors of PyMT mice is potentially a PI3K-mediated phenomenon secondary to *neu* expression.

PI3K up-regulation plays an important role in human breast cancer, particularly in tumors expressing Her-2/neu or Src oncogenes (34), in which PI3K overactivation is associated with antiapoptotic effect. The role of cAMP in breast carcinogenesis is less known. Cox-2 is known to play a role in human breast cancer through promotion of proliferation, angiogenesis, inhibition of apoptosis, and immunosuppression (35). On the other hand, hCG promotes mammary epithelial cell differentiation, and hCG expression by tumor cells is a positive prognostic indicator in human breast cancer (36). However, overexpression of hCG in transgenic mice results in excessive estrogen production by the ovaries, a factor thought to be important in human breast cancer (8). All four transgenic mouse models of breast cancer have primary tumors of variable differentiation with systemic metastases. Up-regulation of signaling pathways in Her-2/neu-, PyMT-, and Cox-2-induced tumors is potentially more representative of the human disease than is up-regulation by marked hCG overexpression.

In this study, we found cAMP and PI3K to be of critical importance in up-regulating NIS in MCF-7 breast cancer cells and transgenic mouse models of breast cancer. Because MCF-7 is the only immortalized cell line with inducible NIS function, it is not known whether the *in vitro* findings are applicable to nonneoplastic immortalized mammary epithelial cells (such as MCF-12A). However, based on the presence of NIS protein in the mammary epithelium of hCG and Her-2/neu transgenic mice before malignant transformation, it is likely that these pathways are operative in normal mammary epithelial cells as well as in breast cancer.

In summary, this study provides several significant advances in the understanding of NIS regulation in breast cancer. First, NIS expression in mammary tumors of Her-2/neu, PyMT, hCGβ, and Cox-2 transgenic mice indicates that signal transduction through cAMP and/or PI3K likely contributes to NIS up-regulation in breast cancer *in vivo*. Furthermore, NIS expression in normal and early hyperplastic lesions of juvenile Her-2/neu mice and in hyperplastic lesions of hCGβ-overexpressing mice indicates that NIS induction is a specific result of transgene expression because NIS is induced before malignant transformation. Second, we demonstrated that activation of cAMP and PI3K induces NIS up-regulation *in vitro* in MCF-7 cells. Previously, all-trans and 9-*cis*-retinoic acid were the only compounds known to increase NIS expression in MCF-7 cells, in which they function through nuclear receptors (37). Finally, NIS expression in these four mouse models provides a vehicle for imaging and therapy using animal models not previously known to have NIS-positive mammary tumors. Further investigation of the molecular mechanisms underlying NIS induction by these two signaling pathways will facilitate NIS-mediated radionuclide therapy for breast cancer becoming a reality.

Acknowledgments

We thank Dr. Ilpo Huhtaniemi (Imperial College London) and Dr. Matti Poutanen (the University of Turku, Turku, Finland) for providing mammary tumor tissue from Ubi-hCGβ transgenic mice; Dr. Jeffrey Rosen, Dr. Darryl Hadsell, and Dr. Dan Medina (Baylor College of Medicine, Houston, TX) for providing mammary tumor tissues from WAP-p53$^{R\rightarrow H}$, WAP-des-IGF-I, p53$^{-/-}$ explants, and bitransgenics; Dr. Susan Rittling (Rutgers University, Piscataway, NJ) for providing mammary tumor tissues from MMTV-c-*myc* × MMTV-v-Ha-ras; Dr. Jeffrey Green [the National Cancer Institute, National Institutes of Health (NIH), Bethesda, MD)] for providing mammary tumor tissues from C3(1)-TAg mice; and Dr. Donna Kusewitt (The Ohio State University, Columbus, OH) for providing mammary tumor tissues from MMTV-PyMT mice. Additionally, we would like to acknowledge Dr. A. F. Parlow (the National Hormone and Peptide Program, Torrance, CA) for providing recombinant hCG for *in vitro* experiments.

Received May 13, 2004. Accepted July 14, 2004.

Address all correspondence and requests for reprints to: Sissy M. Jhiang, 304 Hamilton Hall, 1645 Neil Avenue, Columbus, Ohio 43210. E-mail: jhiang.1@osu.edu.

This work was supported in part by the following grants: NIH NIBIB 1 R01 EB001876-01 and DAMD17-02-1-0119 (to S.M.J.), NIH T32 RR07073 (to K.A.B.K.), and Schering-Plough Research Institute (to C.C.C.).

References

1. **Hortobagyi GN** 1998 Treatment of breast cancer. N Engl J Med 339:974–984
2. **Chlebowski RT** 2000 Reducing the risk of breast cancer. N Engl J Med 343: 191–198
3. **Taurog A** 1996 Hormone synthesis: thyroid iodine metabolism. In: Braverman LE, Utige D, eds. Werner and Ingbar's the thyroid: a fundamental and clinical text. 7th ed. Philadelphia: J.B. Lippincott Co.; 47–81
4. **Carrasco N** 1993 Iodide transport in the thyroid gland. Biochim Biophys Acta 1154:65–82
5. **Tazebay UH, Wapnir IL, Levy O, Dohan O, Zuckier LS, Zhao QH, Deng HF, Amenta PS, Fineberg S, Pestell RG, Carrasco N** 2000 The mammary gland iodide symporter is expressed during lactation and in breast cancer. Nat Med 6:871–878
6. **Wapnir IL, van de Rijn M, Nowels K, Amenta PS, Walton K, Montgomery K, Greco RS, Dohan O, Carrasco N** 2003 Immunohistochemical profile of the sodium/iodide symporter in thyroid, breast, and other carcinomas using high density tissue microarrays and conventional sections. J Clin Endocrinol Metab 88:1880–1888
7. **Kogai T, Kanamoto Y, Che LH, Taki K, Moatamed F, Schultz JJ, Brent GA** 2004 Systemic retinoic acid treatment induces sodium/iodide symporter expression and radioiodide uptake in mouse breast cancer models. Cancer Res 64:415–422
8. **Rulli SB, Ahtiainen P, Makela S, Toppari J, Poutanen M, Huhtaniemi I** 2003 Elevated steroidogenesis, defective reproductive organs, and infertility in transgenic male mice overexpressing human chorionic gonadotropin. Endocrinology 144:4980–4990
9. **Liu CH, Chang SH, Narko K, Trifan OC, Wu MT, Smith E, Haudenschild C, Lane TF, Hla T** 2001 Overexpression of cyclooxygenase-2 is sufficient to induce tumorigenesis in transgenic mice. J Biol Chem 276:18563–18569
10. **Maglione JE, Moghanaki D, Young LJT, Manner CK, Ellies LG, Joseph SO, Nicholson B, Cardiff RD, MacLeod CL** 2001 Transgenic polyoma middle-T mice model premalignant mammary disease. Cancer Res 61:8298–8305
11. **Lin EY, Jones JG, Li P, Zhu L, Whitney KD, Muller WJ, Pollard JW** 2003 Progression to malignancy in the polyoma middle T oncoprotein mouse breast cancer model provides a reliable model for human diseases. Am J Pathol 163:2113–2126
12. **Boggio K, Nicoletti G, Di Carlo E, Cavallo F, Landuzzi L, Melani C, Giovarelli M, Rossi I, Nanni P, De Giovanni C, Bouchard P, Wolf S, Modesti A, Musiani P, Lollini PL, Colombo MP, Forni G** 1998 Interleukin 12-mediated prevention of spontaneous mammary adenocarcinomas in two lines of Her-2/neu transgenic mice. J Exp Med 188:589–596
13. **Guy CT, Webster MA, Schaller M, Parsons TJ, Cardiff RD, Muller WJ** 1992 Expression of the neu protooncogene in the mammary epithelium of transgenic mice induces metastatic disease. Proc Natl Acad Sci USA 89:10578–10582
14. **Ryu KY, Tong Q, Jhiang SM** 1998 Promoter characterization of the Na^+/I^- symporter. J Clin Endocrinol Metab 83:3247–3251
15. **Davis JM, Navolanic PM, Weinstein-Oppenheimer CR, Steelman LS, Hu W, Konopleva M, Blagosklonny MV, McCubrey JA** 2003 Raf-1 and Bcl-2 induce distinct and common pathways that contribute to breast cancer drug resistance. Clin Cancer Res 9:1161–1170
16. **Cho JY, Leveille R, Kao R, Rousset B, Parlow AF, Burak Jr WE, Mazzaferri EL, Jhiang SM** 2000 Hormonal regulation of radioiodide uptake activity and Na^+/I^- symporter expression in mammary glands. J Clin Endocrinol Metab 85:2936–2943
17. **La Perle KMD, Shen D, Buckwalter TLF, Williams B, Haynam A, Hinkle G, Podzerac R, Capen CC, Jhiang SM** 2002 *In vivo* expression and function of the sodium iodide symporter following gene transfer in the MatLyLu rat model of metastatic prostate cancer. Prostate 50:170–178
18. **Kogai T, Schultz JJ, Johnson LS, Huang M, Brent GA** 2000 Retinoic acid induces sodium/iodide symporter gene expression and radioiodide uptake in the MCF-7 breast cancer cell line. Proc Natl Acad Sci USA 97:8519–8524

19. **Rao CV, Li X, Manna SK, Lei ZM, Aggarwal BB** 2004 Human chorionic gonadotropin decreases proliferation and invasion of breast cancer MCF-7 cells by inhibiting NF-κB and AP-1 activation. J Biol Chem 279:25503–25510
20. **Richards JA, Petrel TA, Bruggemeier RW** 2002 Signaling pathways regulating aromatase and cyclooxygenases in normal and malignant breast cells. J Steroid Biochem Mol Biol 80:203–212
21. **Way TD, Kao MC, Lin JK** 2004 Apigenin induces apoptosis through proteasomal degradation of HER2/neu in HER2/neu-overexpressing breast cancer cells via the phosphatidylinositol 3-kinase/Akt-dependent pathway. J Biol Chem 279:4479–4489
22. **Ichaso N, Dilworth SM** 2001 Cell transformation by the middle-T antigen of polyoma virus. Oncogene 20:7908–7916
23. **Planchon P, Veber N, Magnien V, Prévost G, Starzec AB, Israël L** 1995 Evidence for separate mechanisms of antiproliferative action of indomethacin and prostaglandin on MCF-7 breast cancer cells. Life Sci 57:1233–1240
24. **Chang SH, Liu CH, Conway R, Han DK, Nithipatikom K, Trifan OC, Lane TF, Hla T** 2004 Role of prostaglandin E2-dependent angiogenic switch in cyclooxygenase 2-induced breast cancer progression. Proc Natl Acad Sci USA 101:591–596
25. **Arturi F, Lacroix L, Presta I, Scarpelli D, Caillou B, Schlumberge M, Russo D, Bidart JM, Filetti S** 2002 Regulation by human chorionic gonadotropin of sodium/iodide symporter gene expression in the JAr human choriocarcinoma cell line. Endocrinology 143:2216–2220
26. **Arturi F, Presta I, Scarpelli D, Bidart JM, Schlumberger M, Filetti S, Russo D** 2002 Stimulation of iodide uptake by human chorionic gonadotropin in FRTL-5 cells: effects on sodium/iodide symporter gene and protein expression. Eur J Endocrinol 147:655–661
27. **Taki K, Kogai T, Kanamoto Y, Hershman JM, Brent GA** 2002 A thyroid-specific far-upstream enhancer in the sodium/iodide symporter gene requires Pax-8 binding and cyclic adenosine 3′,5′-monophosphate response element-like sequence binding proteins for full activity and is differentially regulated in normal and thyroid cancer cells. Mol Endocrinol 16:2266–2282
28. **Rillema JA, Yu TX, Jhiang SM** 2000 Effect of prolactin on sodium iodide symporter expression in mouse mammary gland explants. Am J Physiol Endocrinol Metab 279:E769–E772
29. **Watson CJ, Burdon TG** 1996 Prolactin signal transduction mechanisms in the mammary gland: the role of Jak/Stat. Rev Reprod 1:1–5
30. **Maus MV, Reilly SC, Clevenger CV** 1999 Prolactin as a chemoattractant for human breast carcinoma. Endocrinology 140:5447–5450
31. **Berrada K, Plesnicher CL, Luo X, Thibonnier M** 2000 Dynamic interaction of human vasopressin/oxytocin receptor subtypes with G protein-coupled receptor kinases and protein kinase C after agonist stimulation. J Biol Chem 275:27229–27237
32. **Cass LA, Meinkoth JL** 2000 Ras signaling through PI3K confers hormone-independent proliferation that is compatible with differentiation. Oncogene 19:924–932
33. **Miller MJ, Rioux L, Prendergast GV, Cannon S, White MA, Meinkoth JL** 1998 Differential effects of protein kinase A on Ras effector pathways. Mol Cell Biochem 18:3718–3726
34. **Fry MJ** 2001 Phosphoinositide 3-kinase signaling in breast cancer: how big a role might it play? Breast Cancer Res 3:305–312
35. **Wang D, Dubois RN** 2004 Cyclooxygenase-2: a potential target in breast cancer. Semin Oncol 31(Suppl 3):64–73
36. **Span PN, Manders P, Heuvel JJ, Thomas CM, Bosch RR, Beex LV, Sweep CG** 2003 Molecular beacon reverse transcription PCR of human chorionic gonadotropin-β-3, -5, and -8 mRNAs has a prognostic value in breast cancer. Clin Chem 49:1074–1080
37. **Tanosaki S, Ikezoe T, Heaney A, Said JW, Dan K, Akashi M, Koeffler HP** 2003 Effect of ligands of nuclear hormone receptor on sodium/iodide symporter expression and activity in breast cancer cells. Breast Cancer Res Treat 79:335–345
38. **Milliken EL, Ameduri RK, Landis MD, Behrooz A, Abdul-Karim FW, Keri RA** 2002 Ovarian hyperstimulation by LH leads to mammary gland hyperplasia and cancer predisposition in transgenic mice. Endocrinology 143:3671–3680
39. **Murphy KL, Rosen JM** 2000 Mutant p53 and genomic instability in a transgenic mouse model of breast cancer. Oncogene 19:1045–1051
40. **Green JE, Shibata M, Yoshidome K, Liu M, Jorcyk C, Anver M, Wigginton J, Wiltrout R, Shibata E, Kaczmarczyk S, Wang W, Liu Z, Calvo A, Couldrey C** 2000 The C3(1)/SV40 T-antigen transgenic mouse model of mammary cancer: ductal epithelial cell targeting with multistage progression to carcinoma. Oncogene 19:1020–1027
41. **Jerry DJ, Kittrell FS, Kuperwasser C, Laucirica R, Dickinson ES, Bonilla PJ, Butel JS, Medina D** 2000 A mammary-specific model demonstrates the role of the p53 tumor suppressor gene in tumor development. Oncogene 19:1052–1058
42. **Hadsell DL, Murphy KL, Bonnette SG, Reece N, Laucirica R, Rosen JM** 2000 Cooperative interaction between mutant p53 and des(1–3)IGF-I accelerates mammary tumorigenesis. Oncogene 19:889–898
43. **Hwang DY, Chae KR, Shin DH, Jang JH, Hwang JH, Kim YJ, Cho JY, Kim BJ, Goo JS, Lim CJ, Kim CK, Cho YY, Paik SG, Cho JS** 2000 Mammary gland tumor in transgenic mice expressing targeted β-casein/HPV16E6 fusion gene. Int J Oncol 17:1093–1098
44. **Zhang M, Shi Y, Magit D, Furth PA, Sager R** 2000 Reduced mammary tumor progression in WAP-TAg/WAP-maspin bitransgenic mice. Oncogene 9:6053–6058
45. **Feng F, Rittling SR** 2000 Mammary tumor development in MMTV-c-*myc*/MMTV-v-Ha-ras transgenic mice is unaffected by osteopontin deficiency. Breast Cancer Res Treat 63:71–79

JCEM is published monthly by The Endocrine Society (http://www.endo-society.org), the foremost professional society serving the endocrine community.

0021-972X/04/$15.00/0
Printed in U.S.A.

The Journal of Clinical Endocrinology & Metabolism 89(5):2344–2350

doi: 10.1210/jc.2003-031963

Application of the Cre/loxP System to Enhance Thyroid-Targeted Expression of Sodium/Iodide Symporter

XIAOQIN LIN, ANDREW H. FISCHER, KWON-YUL RYU, JE-YOEL CHO, THOMAS J. SFERRA, RICHARD T. KLOOS, ERNEST L. MAZZAFERRI, AND SISSY M. JHIANG

Biochemistry Program (X.L., K.-Y.R., S.M.J.), Department of Physiology and Cell Biology (X.L., K.-Y.R., J.-Y.C., S.M.J.), Department of Pediatrics, College of Medicine (T.J.S.), Department of Internal Medicine and Radiology, Divisions of Endocrinology, Diabetes, and Metabolism, and Nuclear Medicine (R.T.K.); Center for Health Outcome Policy Evaluation Studies (E.L.M.), Ohio State University, Columbus, Ohio 43210; Department of Pathology (A.H.F.), University of Massachusetts, Worcester, Massachusetts 01655; Department of Internal Medicine, University of Florida (E.L.M.), Gainesville, Florida 32608-4653; Department of Biological Science (K.-Y.R.), Stanford University, Stanford, California 94305; and Department of Biochemistry (J.-Y.C.), School of Dentistry, Kyungpook National University, Daegu, 700-422, Republic of Korea

Radioiodide uptake activity mediated by the human Na^+/I^- symporter (hNIS) in thyroid follicular cells is the basis for effective ^{131}I therapy in thyroid cancer. However, radioiodide therapy is not effective in patients with thyroid cancer displaying low or absent hNIS expression. This study assessed the Cre/loxP system for enhancing thyroid-targeted hNIS expression driven by the thyroglobulin (Tg) promoter. The following three recombinant adenoviruses (rAd) were constructed: rAd-Tg-hNIS drives hNIS expression by the Tg promoter; rAd-Tg-Cre drives Cre expression by the Tg promoter; and rAd-CMV-loxP-hNIS drives hNIS expression by the cytomegalovirus (CMV) promoter after Cre-mediated excision of an intervening loxP-GFP-Zeo-loxP. Immortalized normal and malignant rat thyroid cell lines and primary cultures of normal human thyroid and human follicular adenoma cells were investigated. We found that the relative promoter activity of Tg *vs.* CMV is critical for the efficacy of the Cre/loxP system. In cells with weak Tg promoter activity, coinfection of rAd-Tg-Cre and rAd-CMV-loxP-hNIS induced higher hNIS expression than single infection of rAd-Tg-hNIS. Finally, Tg promoter activity was partially restored in malignant thyroid cells by forced expression of the paired domain-containing transcription factor (Pax-8), allowing the Cre/loxP system to mildly enhance radioiodide uptake. (*J Clin Endocrinol Metab* 89: 2344–2350, 2004)

THYROID CARCINOMA IS the most common endocrine malignancy, including differentiated thyroid carcinoma (DTC) and undifferentiated (anaplastic) thyroid carcinoma (1). DTC (papillary and follicular carcinoma) comprises about 85–90% of all thyroid malignancies (2). Most patients with DTC can be effectively treated with surgery followed by radioiodide-131 ablation and have a relatively good prognosis (3, 4). However, approximately one third of patients with DTC and all patients with anaplastic carcinoma cannot benefit from radioiodine therapy due to reduced or absent ability to concentrate iodide (2, 5). It has been reported that the loss of radioiodine accumulation in thyroid cancer is due, in part, to decreased expression of the Na^+/I^- symporter (NIS), the key molecule that mediates the active uptake of iodide into thyroid tissues (6–9). Thus, NIS gene transfer to restore and/or increase radioiodide uptake (RAIU) activity represents a promising means to improve the effectiveness of radioiodine therapy in patients with non-iodine-avid thyroid cancers. The objective of this study is to investigate the efficacy of transcriptionally targeted NIS expression in a variety of thyroid cells.

The thyroglobulin (Tg) promoter has been extensively studied for its potential use in transcriptionally targeted thymidine kinase suicide gene therapy of thyroid cancer (10–12). The Tg promoter is an ideal candidate to confer thyroid-targeted gene expression due to its high level of thyroid-specific transcriptional activity. Unfortunately, it has been reported that the Tg promoter activity is weaker in thyroid carcinomas than in normal thyroid tissues (13). A possible way to enhance Tg promoter-driven gene expression in thyroid carcinomas is the application of the Cre/loxP system. Several reports have demonstrated the ability of the Cre/loxP system to enhance transcriptionally targeted suicide gene expression using the Tg promoter or the carcinoembryonic antigen promoter in thyroid or gastrointestinal cancer cells, respectively (11, 14–17).

In this paper, we investigated and compared two different adenoviral systems in providing thyroid-specific human NIS (hNIS) expression (Fig. 1A). The first system involves a single adenovirus, in which hNIS expression is driven by the Tg promoter (rAd-Tg-hNIS). The second system involves two adenoviruses, one in which the Tg promoter drives Cre recombinase expression (rAd-Tg-Cre) and another in which the cytomegalovirus (CMV) promoter is separated from the hNIS gene by two loxP (Cre

Abbreviations: CMV, Cytomegalovirus; DTC, differentiated thyroid carcinoma; FBS, fetal bovine serum; HBSS, Hanks' balanced salt solution; MOI, multiplicity of infection; NIS, Na^+/I^- symporter; rAd, recombinant adenovirus; RAIU, radioiodide uptake; Tg, thyroglobulin.

JCEM is published monthly by The Endocrine Society (http://www.endo-society.org), the foremost professional society serving the endocrine community.

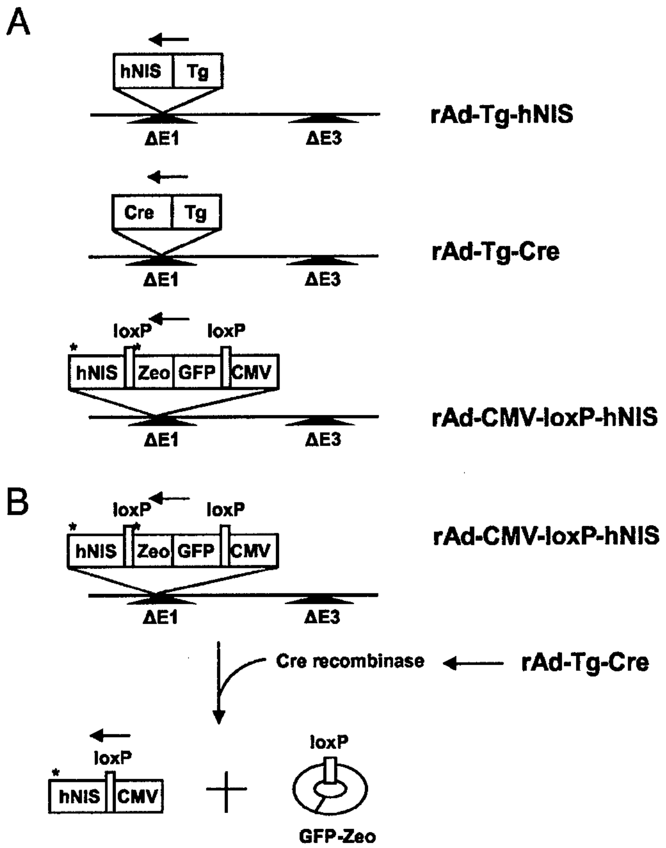

FIG. 1. A, Schematic representation of the E1/E3-deleted adenovirus vector constructs. rAd-Tg-hNIS and rAd-Tg-Cre express hNIS gene and Cre gene, respectively, under the control of the Tg promoter. rAd-CMV-loxP-hNIS is designed to express hNIS gene under the strong CMV promoter only after Cre recombinase excises the GFP-Zeo fusion gene. The ends of the Zeo and hNIS genes both contain a stop codon (*). B, Increased hNIS expression will be induced in cells with an active Tg promoter by the Tg-Cre/CMV-loxP-hNIS system. Cre recombinase excises GFP-Zeo fusion gene between the two loxP sites as a covalently closed circle, leaving one loxP site behind and allowing transcription of hNIS driven by the strong CMV promoter.

recombinase recognition) sites (rAd-CMV-loxP-hNIS). Coinfection of these two adenoviruses into thyroid cells results in Cre expression, which then excises an intervening DNA sequence bearing a stop codon between the two loxP sites, thereby allowing hNIS expression under control of the strong CMV promoter (Fig. 1B). Here, we show that the relative promoter activity of Tg *vs.* CMV is critical for the ability of the Cre/loxP system to enhance thyroid-targeted hNIS expression. Thus, in cells with weak Tg promoter activity, coinfection of rAd-Tg-Cre and rAd-CMV-loxP-hNIS induced higher hNIS expression than single infection of rAd-Tg-hNIS.

Materials and Methods

Cell lines and stable clones

Cos-7 monkey kidney cells were maintained in DMEM supplemented with 10% fetal bovine serum (FBS). FRTL-5 differentiated normal rat thyroid cells (kindly provided by Dr. Leonard D. Kohn, Ohio University, Athens, OH) were cultured in Coon's modified Ham's F-12 medium, supplemented with 5% calf serum and six hormone (6H) mixture as described previously (18). Malignant FRTC cells were derived from FRTL-5 cells transformed with muramyl dipeptide (kindly provided by Dr. Makoto Iitaka, Saitama Medical School, Saitama, Japan) and maintained in the same medium as FRTL-5 cells.

Malignant FRTC cells were stably transfected with 5 μg rat paired domain-containing transcription factor (Pax-8)/pcDNA$_3$ (our unpublished data) by calcium phosphate transfection. The DNA precipitates were replaced with fresh medium 6 h later. FRTC/Pax-8 cells were selected with 320 μg/ml of geneticin (G-418) 48 h posttransfection. The selected clones were then screened for the level of Pax-8 protein by Western blot analysis (data not shown).

Preparation of human normal or tumor primary thyroid culture

Human normal thyroid tissue and human follicular adenoma tissue were put into tissue culture as described previously with minor modification (19). Fresh tissue (0.1–1 g) was cut into approximately 1-mm cubes and washed with cold Hanks' Balanced Salt Solution (HBSS; calcium and magnesium free). The tissue was then digested with digestion solution [fresh clostridium collagenase (100 U/ml) and Dispase (1 mg/ml) in HBSS] for 1.5 h at 37 C with 5% CO_2 and agitated with a large bore pipette every 30 min. The large undigested fragments were allowed to settle briefly, and the supernatant containing released epithelial clusters was transferred to a fresh flask with the addition of 10% FBS and maintained at 37 C. The remaining tissue fragments continued to be digested by incubating with fresh digestion solution at 37 C until the digested tissue became very soft and filmy. This entire sample and the previously collected supernatant were filtered through a 70-mm falcon cell strainer to remove the remaining clumps that consist largely of connective tissue. The cells were then washed with HBSS three times and cultured in a 2:1:1 mixture of DMEM, Ham's F-12, and MCDB-104 (Life Technologies, Inc., Paisley, UK) supplemented with 10% FBS. Human Investigation Committee approval for these studies was obtained at the University of Massachusetts (Institutional Review Board no. H-10396).

Construction and production of rAd

The plasmid pSh-Tg-hNIS was constructed as follows. A *Kpn*I-*Pme*I fragment containing the hNIS gene was excised from pSh-CMV-hNIS (20) and cloned into the pShuttle vector. The 2.0-kb bovine Tg promoter (located from −2036 to +9 nucleotide relative to the transcriptional start site) was then released as a *Spe*I-*Kpn*I fragment from pSh-Tg-PTC3 and inserted upstream of the hNIS gene to generate pSh-Tg-hNIS.

The plasmid pSh-Tg-Cre was constructed as follows. The Cre recombinase gene and 588 bp of polyA sequence from the PBS185 vector were released as a *Spe*I (blunt-ended by T_4 DNA polymerase)-*Xba*I fragment and replaced the hNIS gene in pSh-Tg-hNIS. The extra 588-bp polyA fragment was then removed by *Mlu*I/*Xba*I digestion to generate pSh-Tg-Cre.

The plasmid pSh-CMV-loxP-hNIS was constructed as follows. The loxP-GFP-Zeo-loxP fragment from the pCMV-β-4-REV vector was subcloned as a *Not*I (blunt-ended by T_4 DNA polymerase) fragment into the *Kpn*I site of pSh-CMV-hNIS.

rAd-Tg-hNIS, rAd-Tg-Cre, and rAd-CMV-loxP-hNIS were produced and purified as described previously (20, 21). The titers of adenoviruses were determined by plaque formation in 293 cells and expressed in pfu/ml.

Detection of hNIS protein by Western blot analysis

Cells were plated in 100-mm dishes. When cells became 70–80% confluent, they were infected with various adenoviruses at the indicated multiplicity of infection (MOI) for 2 h. Forty-eight hours postinfection, cells were harvested for Western blot analysis as described previously with minor modification (22). Briefly, the membrane fractions of the cells were subjected to 7.5% SDS-PAGE. The proteins were transferred to nitrocellulose membrane (Schleicher & Schuell, Keene, NH). The membrane was incubated with the affinity-purified hNIS antibody (1:1500), which recognizes the COOH terminus of hNIS protein, for 1 h at room temperature, followed by incubation with horseradish peroxidase-conjugated donkey α-rabbit IgG (1:4000) (Amersham Pharmacia, Piscataway, NJ) for 1 h at room temperature. The filter was incubated with the enhanced chemiluminescence detection reagents (Amersham) for 1 min and exposed to x-ray film.

Detection of NIS function by RAIU assay

Cells were seeded in 24-well plates. When cells became 70–80% confluent, they were incubated with various adenoviruses at the indicated MOI for 2 h. Forty-eight hours postinfection, RAIU assay was performed as described previously (20). Briefly, cells were incubated with 2 μCi Na ^{125}I for 30 min at 37 C with 5% CO_2. Cells were then washed with cold HBSS twice, and the radioiodide taken up by the cells was released by 95% ethanol for 20 min at room temperature. The radioactivity was counted by a γ-counter (Packard Instruments, Downers Grove, IL). Experiments were performed in triplicate.

Detection of the promoter activities of CMV and Tg by luciferase assay

Cells were seeded in six-well plate. When cells became 50–60% confluent, calcium phosphate transfection or FuGENE 6 transfection (Roche, Nutley, NJ) was performed using 3 μg of Tg/pGL$_2$B (18) or CMV/pGL$_2$B (our unpublished data), in which Tg or CMV promoter was inserted upstream of the promoterless luciferase reporter gene in pGL$_2$B vector, respectively. CMV/β-galactosidase DNA construct (0.2 μg) was cotransfected with each DNA construct to normalize the transfection efficiency. The DNA precipitates were replaced with fresh medium 6 h later for calcium phosphate transfection. Forty-eight hours posttransfection, the cells were lysed with 80 μl lysis buffer provided in the luciferase assay kit (Promega Corporation, Madison, WI). The luciferase and β-galactosidase assays were carried out as described previously (18). Experiments were performed in duplicate.

Results

Generation of functional rAds: rAd-Tg-hNIS, rAd-Tg-Cre, and rAd-CMV-loxP-hNIS

Three rAds, rAd-Tg-hNIS, rAd-Tg-Cre, and rAd-CMV-loxP-hNIS, were constructed as described in *Materials and Methods*. To verify the function of these three rAds, various adenoviruses were infected into FRTL-5 rat normal thyroid cells or Cos-7 monkey kidney cells. The level of hNIS protein in infected cells was detected by Western blot analysis. As expected, rAd-Tg-hNIS can only express hNIS protein in Tg-expressing FRTL-5 cells but not in Cos-7 cells (Fig. 2A). Similarly, hNIS expression was detected only in FRTL-5 cells but not in Cos-7 cells after coinfection with rAd-Tg-Cre and rAd-CMV-loxP-hNIS (Fig. 2B). The cells infected with rAd-CMV-loxP-hNIS alone did not induce hNIS expression, indicating that Cre recombinase is required for hNIS expression in the dual virus system (Fig. 2B). It is notable that although FRTL-5 cells express endogenous rat NIS (rNIS), our hNIS antibodies do not cross-react with rNIS (see lane 3 in Fig. 2B).

Enhanced hNIS expression and RAIU activity in FRTL-5 rat normal thyroid cells coinfected with rAd-Tg-Cre and rAd-CMV-loxP-hNIS

To compare the abilities of the Tg-hNIS and Tg-Cre/CMV-loxP-hNIS systems to mediate hNIS expression and function, we infected FRTL-5 cells with either rAd-Tg-hNIS alone (MOI = 20) or with both rAd-Tg-Cre and rAd-CMV-loxP-hNIS (MOI = 10:10). Analysis of coinfection with the Cre/loxP system revealed that optimal hNIS

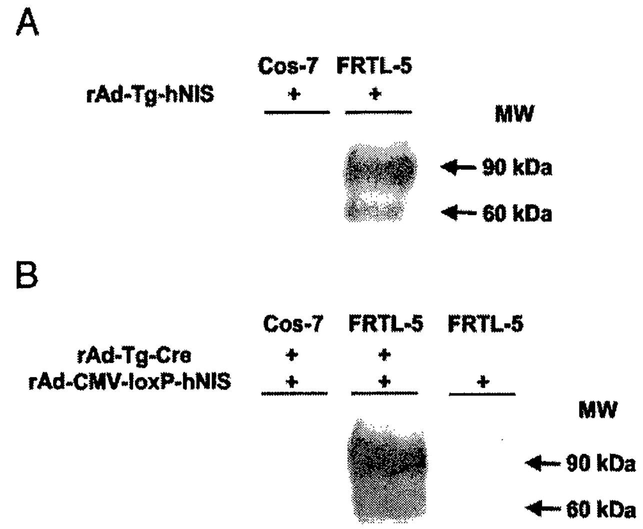

FIG. 2. The three adenoviruses were functional in cultured cells by Western blot analysis of hNIS protein. A, rAd-Tg-hNIS (MOI = 10) conferred hNIS expression only in differentiated FRTL-5 thyroid cells that express Tg but not in Cos-7 monkey kidney cells. The figure shown was taken with 3 min of exposure. B, Coinfection of rAd-Tg-Cre and rAd-CMV-loxP-hNIS (MOI = 10:10) only induced hNIS expression in FRTL-5 cells but not in Cos-7 cells. rAd-CMV-loxP-hNIS (MOI = 20) alone did not induce hNIS expression in FRTL-5 cells, indicating that Cre recombinase is required for hNIS expression in the dual virus system. The figure shown was taken with 10 sec of exposure. Five-microgram membrane fractions were loaded for each lane. Note the mature hNIS glycoprotein (90 kDa) and the partially glycosylated hNIS protein (60 kDa). MW, Molecular weight.

expression occurred when cells were administered with a 1:1 ratio of rAd-Tg-Cre *vs.* rAd-CMV-loxP-hNIS (data not shown). Because hNIS antibodies do not detect endogenous rNIS in FRTL-5 cells, we were able to compare the expression levels of hNIS induced by the designated adenovirus. Our data showed that both Tg-hNIS and Tg-Cre/CMV-loxP-hNIS induced hNIS expression in FRTL-5 cells; however, the level of hNIS protein in FRTL-5 cells coinfected with the Tg-Cre/CMV-loxP-hNIS system was significantly higher than that in cells infected with rAd-Tg-hNIS alone (Fig. 3A). It is difficult to quantify the relative hNIS expression levels induced by one system *vs.* another because different exposure times were required to optimize the detection of hNIS protein.

As shown in Fig. 3B, the RAIU activity in FRTL-5 cells was significantly increased by infection of rAd-Tg-hNIS alone as well as by coinfection of rAd-Tg-Cre and rAd-CMV-loxP-hNIS. Interestingly, although Tg-Cre/CMV-loxP-hNIS is much more efficient than Tg-hNIS in inducing hNIS expression, the increase of RAIU activity in cells coinfected with the Tg-Cre/CMV-loxP-hNIS system was only slightly higher than that in cells infected with rAd-Tg-hNIS alone (Fig. 3B). Thus, it appears that not all induced hNIS resulted in increasing RAIU activity in infected FRTL-5 cells. This may be because noninfected FRTL-5 cells already have high-level iodide uptake due to endogenous rNIS (see *Discussion*).

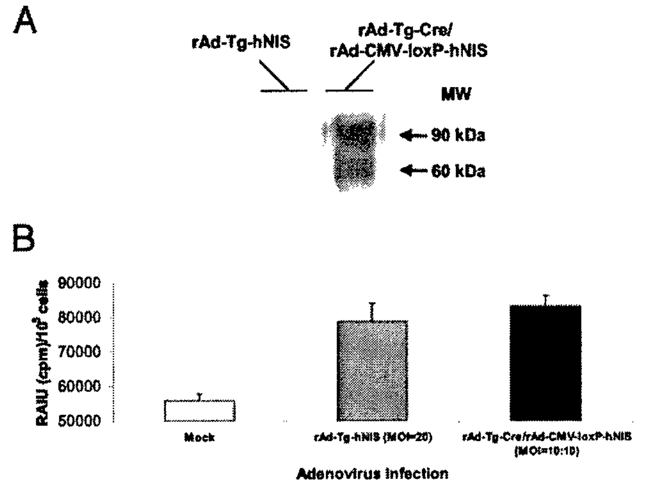

FIG. 3. Coinfection of rAd-Tg-Cre and rAd-CMV-loxP-hNIS (MOI = 10:10) enhanced hNIS expression and RAIU activity in FRTL-5 cells compared with single infection of rAd-Tg-hNIS (MOI = 20). A, Western blot analysis of hNIS expression (0.5 μg per lane). The hNIS expression level in cells coinfected with rAd-Tg-Cre/rAd-CMV-loxP-hNIS was much higher than that in cells infected with rAd-Tg-hNIS. Thus, different exposure times were required to optimize the detection of hNIS protein induced by the Tg-hNIS and Tg-Cre/CMV-loxP-hNIS systems. The figure shown was taken with 1 min of exposure. MW, Molecular weight. B, RAIU assay for NIS function (the sum of endogenous rNIS and exogenous hNIS activities). The noninfected FRTL-5 cells served as a control. The same passage of FRTL-5 cells (P23) was used for Western blot analysis and RAIU assay.

Enhanced hNIS expression and RAIU activity in FRTC/Pax-8 rat malignant thyroid cells coinfected with rAd-Tg-Cre and rAd-CMV-loxP-hNIS

Malignant FRTC thyroid cells are reported to express low levels of Tg mRNA (10, 23), which is similar to less differentiated thyroid tumors. However, hNIS expression was not detectable by Western blot analysis in malignant FRTC cells infected with either rAd-Tg-hNIS alone or rAd-Tg-Cre and rAd-CMV-loxP-hNIS (data not shown). Our luciferase assay showed that malignant FRTC cells had extremely weak, if any, Tg promoter activity (data not shown). It has been reported that the reintroduction of a thyroid-specific transcription factor, Pax-8, into PCPy cells, which are derived from the differentiated PC Cl 3 immortalized rat thyroid cells transformed with polyoma middle T antigen, was sufficient to increase Tg promoter activity (24). Therefore, we stably transfected rat Pax-8 into malignant FRTC cells (FRTC/Pax-8) to increase Tg promoter activity. As shown in Fig. 4A, hNIS expression in FRTC/Pax-8 cells coinfected with rAd-Tg-Cre/rAd-CMV-loxP-hNIS (MOI = 20:20) was higher than that of cells infected with rAd-Tg-hNIS alone (MOI = 40). In cells infected with the Cre/loxP system (MOI = 25:25), the RAIU mediated by exogenous hNIS was higher than in cells infected with rAd-Tg-hNIS (MOI = 50; Fig. 4B). We also observed a slight increase in background RAIU in FRTC stably transfected with Pax-8 compared with FRTC parental cells (data not shown). This increase may be due to the direct stimulating effect of Pax-8 on the endogenous rNIS promoter. It is noteworthy that the RAIU activity in FRTC/Pax-8 cells (Fig. 4B) is much lower than that in FRTL-5 cells (Fig. 3B).

Enhanced RAIU activity in normal human thyroid primary culture coinfected with rAd-Tg-Cre and rAd-CMV-loxP-hNIS

Short-term primary cultures of normal human thyrocytes serve as a physiologic *in vitro* model. To evaluate the efficacy of the Tg-Cre/CMV-loxP-hNIS system in the primary culture of human normal thyrocytes, cells were either infected with rAd-Tg-hNIS alone (MOI = 20) or coinfected with rAd-Tg-Cre and rAd-CMV-loxP-hNIS (MOI = 10:10). Only RAIU assay was performed to investigate hNIS function due to the availability of cell numbers. As shown in Fig. 5, the RAIU activity was increased by both systems, and the increase of RAIU activity in cells coinfected with Tg-Cre/CMV-loxP-hNIS was significantly higher than that in cells infected with rAd-Tg-hNIS alone. Similarly to FRTL-5 cells, the primary culture infected with control adenovirus displayed a rela-

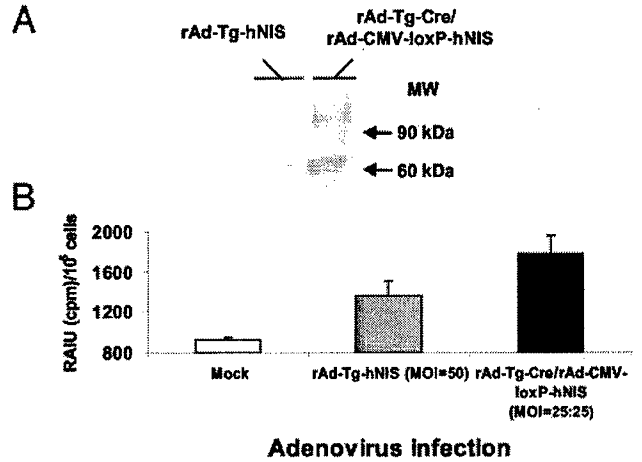

FIG. 4. Coinfection of rAd-Tg-Cre and rAd-CMV-loxP-hNIS enhanced hNIS expression and RAIU activity in FRTC malignant thyroid cells stably transfected with Pax-8 compared with single infection with rAd-Tg-hNIS. A, Western blot analysis of hNIS expression in cells either infected with rAd-Tg-hNIS (MOI = 40) or coinfected with rAd-Tg-Cre and rAd-CMV-loxP-hNIS (MOI = 20:20; 100 μg per lane). The figure shown was taken with 2 min of exposure. MW, Molecular weight. B, RAIU assay for NIS function in cells either infected with rAd-Tg-hNIS (MOI = 50) or coinfected with rAd-Tg-Cre and rAd-CMV-loxP-hNIS (MOI = 25:25). Noninfected FRTC/Pax-8 cells served as a control.

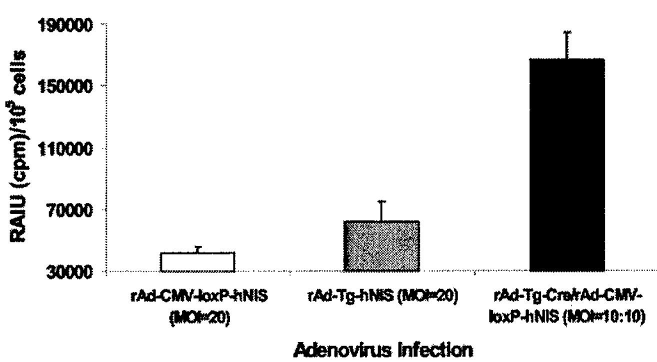

FIG. 5. Coinfection of rAd-Tg-Cre and rAd-CMV-loxP-hNIS (MOI = 10:10) significantly enhanced RAIU activity in normal human thyroid primary culture compared with single infection of rAd-Tg-hNIS (MOI = 20). Cells infected with rAd-CMV-loxP-hNIS (MOI = 20) alone served as a control for endogenous hNIS.

tively high level of iodide uptake, which is due to the expression of endogenous hNIS protein in the normal primary culture.

Enhanced hNIS expression and RAIU activity in human thyroid follicular adenoma primary culture coinfected with rAd-Tg-Cre and rAd-CMV-loxP-hNIS

A human thyroid follicular adenoma primary culture was derived from a thyroid follicular adenoma that was cold on the radioiodide scan 3 months before surgery, which implies the absent or weak hNIS expression or function in the cells compared with surrounding normal cells. To reintroduce hNIS expression and evaluate the efficacy of the Tg-Cre/CMV-loxP-hNIS system in this follicular adenoma, cultured cells were either infected with rAd-Tg-hNIS alone (MOI = 20) or coinfected with rAd-Tg-Cre and rAd-CMV-loxP-hNIS (MOI = 10:10). Western blot analysis and RAIU assay were performed to examine hNIS expression and hNIS function. Again, as shown in Fig. 6, hNIS expression levels and the increase of RAIU activity induced by Tg-Cre/CMV-loxP-hNIS (MOI = 10:10) were significantly higher than those induced by rAd-Tg-hNIS alone (MOI = 20). The cells infected with rAd-CMV-loxP-hNIS alone (MOI = 20) showed low RAIU activity.

Relative promoter activity of Tg vs. CMV in targeted thyroid cells crucial for the efficacy of the Tg-Cre/CMV-loxP-hNIS system

In this paper, we hypothesize that the Tg-Cre/CMV-loxP-hNIS system is able to enhance thyroid-targeted hNIS expression. The hypothesis is mainly based on the assumption that CMV promoter activity is much stronger than Tg promoter activity in targeted cells. Thus, the relative promoter activity of Tg *vs.* CMV in the targeted cells will be vital for the efficacy of Tg-Cre/CMV-loxP-hNIS. Experiments were performed to correlate the relative promoter activity of Tg *vs.* CMV with the efficacy of Tg-Cre/CMV-loxP-hNIS in targeted thyroid cells. The investigated cells were divided into four experimental groups. Cells were either transfected with Tg/pGL$_2$B or CMV/pGL$_2$B to determine Tg or CMV promoter activity by luciferase assay. Simultaneously, cells were either infected with rAd-Tg-hNIS alone (MOI = 20) or coinfected with the Tg-Cre/CMV-loxP-hNIS system (MOI = 10:10) to determine RAIU activity. As shown in Fig. 7, when the relative promoter activity of Tg *vs.* CMV is 1:5 in P14 FRTL-5 cells, Cre/loxP is not effective to further enhance Tg-targeted hNIS-mediated RAIU activity. In comparison, when Tg promoter activity was much weaker than CMV promoter activity in P20 FRTL-5 (the relative promoter activity of Tg *vs.* CMV is 1:333), the Cre/loxP system was more effective in increasing RAIU activity than Tg-hNIS alone. In primary cultures of human thyrocytes, in which the relative promoter activity of Tg *vs.* CMV was about 1:1600 or 1:1500, the Tg-Cre/CMV-loxP-hNIS system was very effective in enhancing Tg-targeted hNIS-mediated RAIU activity (Fig. 7). In addition, it was interesting to note that the CMV promoter activity varied among different cells (data not shown).

Discussion

Several groups have investigated the potential of NIS-mediated radionuclide imaging and therapy in thyroid or nonthyroidal cancer cells (5, 25, 26). However, most studies express NIS under the control of the strong and constitutive CMV promoter as proof-of-principle experiments. To apply NIS-based gene therapy to patients, it is important to restrict NIS expression to targeted cells to avoid unwanted side effects in nontargeted tissues. For patients after total thyroidectomy, NIS expression may be restricted to residual thyroid cancer using Tg as a tissue-specific promoter. However, Tg promoter activity is generally much weaker than that of a constitutive viral promoter. Thus, the Tg-Cre/CMV-loxP-hNIS system may be superior to a Tg-hNIS system to induce hNIS expression in thyroidal tissues. In this study, we showed that the Cre/loxP system was effective in enhancing

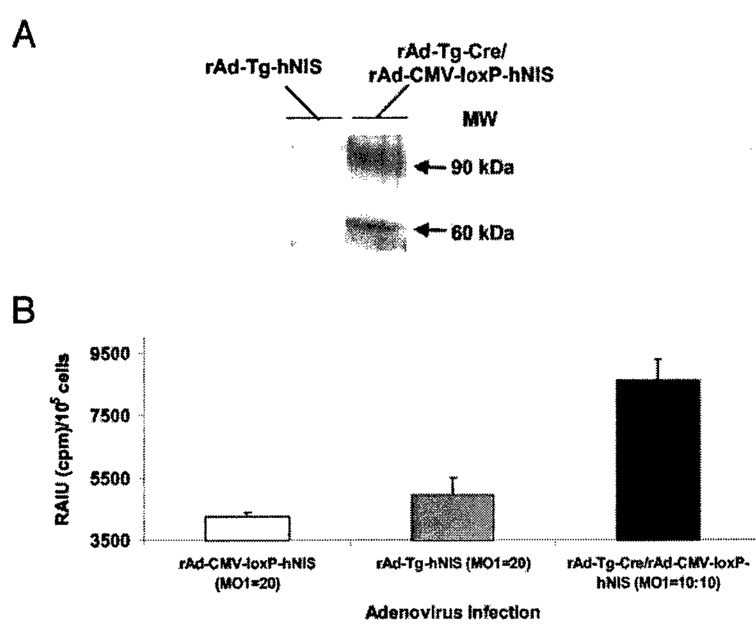

FIG. 6. Coinfection of rAd-Tg-Cre and rAd-CMV-loxP-hNIS (MOI = 10:10) enhanced hNIS expression and RAIU activity in human thyroid follicular adenoma primary culture compared with single infection of rAd-Tg-hNIS (MOI = 20). A, Western blot analysis of hNIS expression (30 μg per lane). The figure shown was taken with 2 min of exposure. MW, Molecular weight. B, RAIU assay for NIS function. Cultured cells infected with rAd-CMV-loxP-hNIS (MOI = 20) alone served as a control.

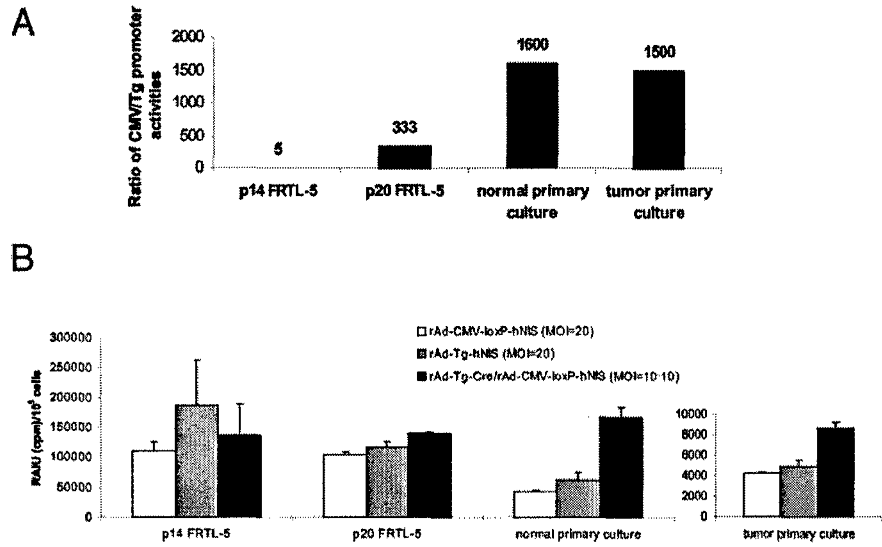

FIG. 7. Relative promoter activity of Tg *vs.* CMV in targeted thyroid cells is crucial for the efficacy of the Tg-Cre/CMV-loxP-hNIS system. (A) Relative promoter activity of Tg *vs.* CMV in P14 FRTL-5 cells, P20 FRTL-5 cells, normal human thyroid primary culture, and human thyroid follicular adenoma primary culture. Tg/pGL$_2$B or CMV/pGL$_2$B was transfected into targeted thyroid cells separately to analyze Tg promoter and CMV promoter activity, respectively. The luciferase activity of CMV/pGL$_2$B was reported relative to the luciferase activity of Tg/pGL$_2$B, which was arbitrarily designated as 1. All experiments were performed in duplicate. (B) RAIU assay for NIS function in targeted thyroid cells either infected with rAd-CMV-loxP-hNIS (MOI = 20) alone, rAd-Tg-hNIS (MOI = 20) alone, or coinfected with rAd-Tg-Cre and rAd-CMV-loxP-hNIS (MOI = 10:10).

transcriptionally targeted NIS expression/function in FRTL-5 cells, FRTC cells, normal human thyroid primary culture, and human thyroid follicular adenoma primary culture. In addition, we showed that the efficacy of Tg-Cre/CMV-loxP-hNIS is dependent upon the relative promoter activity of Tg *vs.* CMV. Thus, for thyroid cancers with strong Tg promoter activity, a Tg-hNIS system may be sufficient to confer high levels of hNIS expression to improve radioiodide therapy. For thyroid cancers with weak Tg promoter activity, Cre/loxP is an attractive system to enhance Tg-targeted NIS expression. However, for thyroid cancers with negligible Tg promoter activity, strategies to increase Tg promoter activity must also be used to confer Tg-targeted hNIS expression.

Immortalized FRTL-5 cells have been known to display different characteristics with age or transformation. Serially passaged FRTL-5 cells are reported to dedifferentiate and lose Tg expression (27). This is consistent with our data that the aged P20 FRTL-5 cells had weaker Tg promoter activity than the young P14 FRTL-5 cells (Fig. 7A). Similarly, decreased Tg promoter activity has been reported in FRTC tumor of the 12th generation compared with the third generation (23). Although forced expression of Pax-8 in FRTC cells increased Tg promoter activity and allowed Tg-targeted hNIS expression/function, the increase of RAIU activity in FRTC/Pax-8 cells coinfected with Tg-Cre/CMV-loxP-hNIS was not high enough to justify further animal study. We also evaluated the effects of Cre/loxP system on FTC133 human thyroid carcinoma cells (28). However, FTC133 cells exhibited undetectable Tg promoter activities and did not induce RAIU activity by the Tg-hNIS system or the Cre/loxP system (data not shown). Therefore, a non-iodine-avid tumorigenic thyroid tumor cell line, yet with some retained Tg promoter activity, will be essential to examine the efficacy of the Cre-loxP system to increase Tg-targeted hNIS expression/function in preclinical animal models.

It is interesting to note that the extent of increased RAIU activity does not appear to be proportional to the extent of induced hNIS expression in all cells studied. For cells with high levels of endogenous NIS expression and function, it is possible that the cell surface is eventually saturated with functional NIS, excluding further cell surface trafficking of exogenous hNIS. However, for cells with low or absent endogenous NIS, defects in cell surface trafficking of hNIS are suspected. The proper and efficient cell surface trafficking has been shown to play an important role in the functional expression of hNIS in thyroid cells (9, 29, 30). Thus, possible defects in cell surface trafficking of hNIS in malignant cells remain a real challenge for hNIS-based gene therapy.

To apply Tg-targeted NIS gene therapy, Tg promoter activity in cancer cells needs to be sufficient, if not maximized. In this study, we showed that forced expression of Pax-8 into FRTC cells slightly increased Tg promoter activity and induced detectable hNIS expression. Thyroid transcription factor 1 (TTF-1) has also been shown to reactivate the Tg promoter in thyroid carcinoma cells (31, 32). Therefore, forced expression of both TTF-1 and Pax-8 may further facilitate the efficacy of Tg-targeted NIS gene therapy. In addition, a tandem repeat of the minimal Tg promoter has been shown to induce much higher thymidine kinase expression in transduced thyroid cells than the single Tg promoter did (33). Thus, it is desirable to generate a composite Tg promoter yielding the highest thyroid-specific promoter activity. Furthermore, the efficiency of Cre-directed site-specific recombination could be enhanced by facilitating Cre nuclear localization (34). Finally, the efficacy of the Cre/loxP system may be further improved by dually expressing Tg-Cre and CMV-loxP-hNIS in a single adenovirus to avoid inefficient coinfection of two adenoviruses.

In conclusion, the Tg-Cre/CMV-loxP-hNIS system can significantly enhance thyroid-targeted hNIS expression and induce RAIU activity in thyroid cells with weak Tg promoter activity. We showed that the relative promoter activity of Tg *vs.* CMV is crucial for the efficacy of the Cre/loxP system. Thus, before NIS-based gene therapy, Tg promoter activity should be evaluated, for example, by measuring serum Tg levels upon TSH stimulation in patients.

Acknowledgments

We thank Dr. Leonard D. Kohn at Ohio University (Athens, OH) for providing FRTL-5 cells; Dr. Makoto Iitaka at Saitama Medical School

(Saitama, Japan) for providing FRTC cells; Dr. Yuji Nagayama at Nagasaki University (Nagasaki, Japan) for helpful discussion about FRTC cells; and Mr. Derek K. Marsee for support in manuscript preparation.

Received November 12, 2003. Accepted February 11, 2004.

Address all correspondence and requests for reprints to: Sissy M. Jhiang, Ph.D., The Ohio State University, Department of Physiology and Cell Biology, 304 Hamilton Hall, 1645 Neil Avenue, Columbus, Ohio 43210. E-mail: Jhiang.1@osu.edu.

This work was supported in part by Department of Defense Prostate Cancer Research Program DAMD 17-02-0119 (to S.M.J.).

References

1. **Gimm O** Thyroid cancer. Cancer Lett 163:143–156, 2001
2. **Mazzaferri EL, Jhiang SM** 1994 Differentiated thyroid cancer long-term impact of initial therapy. Trans Am Clin Climatol Assoc 106:151–168; discussion 168–170
3. **Mazzaferri EL** 1996 Radioiodine and other treatments and outcomes. In: Braverman LE, Utiger RD, eds. Werner and Ingbar's the thyroid: a fundamental and clinical text. New York: Lippincott-Raven; 922–945
4. **Wartofsky L, Sherman SI, Gopal J, Schlumberger M, Hay ID** 1998 The use of radioactive iodide in patients with papillary and follicular thyroid cancer. J Clin Endocrinol Metab 83:4195–4203
5. **Chung JK** 2002 Sodium iodide symporter: its role in nuclear medicine. J Nucl Med 43:1188–1200
6. **Arturi F, Russo D, Schlumberger M, du Villard JA, Caillou B, Vigneri P, Wicker R, Chiefari E, Suarez HG, Filetti S** 1998 Iodide symporter gene expression in human thyroid tumors. J Clin Endocrinol Metab 83:2493–2496
7. **Calliou B, Troalen F, Baudin E, Talbot M, Filetti S, Schlumberger M, Bidart JM** 1998 Na+/I- symporter distribution in human thyroid tissues: an immunohistochemical study. J Clin Endocrinol Metab 83:4102–4106
8. **Lazar V, Bidart JM, Caillou B, Mahe C, Lacroix L, Filetti S, Schlumberger M** 1999 Expression of the Na^+/I^- symporter gene in human thyroid tumors: a comparison study with other thyroid-specific genes. J Clin Endocrinol Metab 84:3228–3234
9. **Dohan O, De la Vieja A, Paroder V, Riedel C, Artani M, Reed M, Ginter CS, Carrasco N** 2003 The sodium/iodide symporter (NIS): characterization, regulation, and medical significance. Endocr Rev 24:48–77
10. **Braiden V, Nagayama Y, Iitaka M, Namba H, Niwa M, Yamashita S** 1998 Retrovirus-mediated suicide gene/prodrug therapy targeting thyroid carcinoma using a thyroid-specific promoter. Endocrinology 139:3996–3999
11. **Nagayama Y, Nishihara E, Iitaka M, Namba H, Yamashita S, Niwa M** 1999 Enhanced efficacy of transcriptionally targeted suicide gene/prodrug therapy for thyroid carcinoma with the Cre-loxP system. Cancer Res 59:3049–3052
12. **Zhang R, Straus FH, DeGroot LJ** 2001 Adenoviral-mediated gene therapy for thyroid carcinoma using thymidine kinase controlled by thyroglobulin promoter demonstrates high specificity and low toxicity. Thyroid 11:115–123
13. **Fabbro D, Di Loreto C, Beltrami CA, Belfiore A, Di Lauro R, Damante G** 1994 Expression of thyroid-specific transcription factors TTF-1 and PAX-8 in human thyroid neoplasms. Cancer Res 54:4744–4749
14. **Kijima T, Osaki T, Nishino K, Kumagai T, Funakoshi T, Goto H, Tachibana I, Tanio Y, Kishimoto T** 1999 Application of the Cre recombinase/loxP system further enhances antitumor effects in cell type-specific gene therapy against carcinoembryonic antigen-producing cancer. Cancer Res 59:4906–4911
15. **Goto H, Osaki T, Kijima T, Nishino K, Kumagai T, Funkoshi T, Kimura H, Takeda Y, Yoneda T, Tachibana I, Hayashi S** 2001 Gene therapy utilizing the Cre/loxP system selectively suppresses tumor growth of disseminated carcinoembryonic antigen-producing cancer cells. Int J Cancer 94:414–419
16. **Ueda K, Iwahashi M, Nakamori M, Nakamura M, Matsuura I, Yamaue H, Tanimura H** 2001 Carcinoembryonic antigen-specific suicide gene therapy of cytosine deaminase/5-fluorocytosine enhanced by the Cre/loxP system in the orthotopic gastric carcinoma model. Cancer Res 61:6158–6162
17. **Ueda K, Iwahashi M, Nakamori M, Nakamura M, Matsuura I, Ojima T, Yamaue H** 2003 Improvement of carcinoembryonic antigen-specific prodrug gene therapy for experimental colon cancer. Surgery 133:309–317
18. **Tong Q, Ryu KY, Jhiang SM** 1997 Promoter characterization of the rat Na+/I-symporter gene. Biochem Biophys Res Commun 239:34–41
19. **Bond J, Dawson T, Lemoine N, Wynford-Thomas D** 1992 Effect of serum growth factors and phorbol ester on growth and survival of human thyroid epithelial cells expressing mutant ras. Mol Carcinog 5:129–135
20. **Cho JY, Xing S, Liu X, Buckwalter TLF, Hwa L, Sferra TJ, Chiu IM, Jhiang SM** 2000 Expression and activity of human Na+/I- symporter in human glioma cells by adenovirus-mediated gene delivery. Gene Ther 7:740–749
21. **He TC, Zhou S, da Costa LT, Yu J, Kinzler KW, Vogelstein B** 1998 A simplified system for generating recombinant adenovirus. Proc Natl Acad Sci USA 95: 2509–2514
22. **Jhiang SM, Cho JY, Ryu KY, DeYoung BR, Smanik PA, McGaughy VR, Fischer AH, Mazzaferri EL** 1998 An immunohistochemical study of Na^+/I^- symporter in human thyroid tissues and salivary gland tissues. Endocrinology 139:4416–4419
23. **Iitaka M, Fukasawa N, Kitahama S, Miura S, Kawakami Y, Sato H, Sugano S, Ishii J, Katayama S** 1997 Transplantable rat thyroid cancer cell line FRTC transformed with muramyl dipeptide. Br J Cancer 75:40–46
24. **Pasca di Magliano M, Di Lauro R, Zannini M** 2000 Pax8 has a key role in thyroid cell differentiation. Proc Natl Acad Sci USA 97:13144–13149
25. **Shimura H, Haraguchi K, Miyazaki A, Endo T, Onaya T** 1997 Iodide uptake and experimental 131I therapy in transplanted undifferentiated thyroid cancer cells expressing the Na/I symporter gene. Endocrinology 138:4493–4496
26. **Cho JY, Shen DH, Yang W, Williams B, Buckwalter TL, La Perle KM, Hinkle G, Pozderac R, Kloos R, Nagaraja HN, Barth RF, Jhiang SM** 2002 In vivo imaging and radioiodine therapy following sodium iodide symporter gene transfer in animal model of intracerebral gliomas. Gene Ther 9:1139–1145
27. **Zimmermann-Belsing T, Rasmussen AK, Feldt-Rasmussen U** 1998 Lack of thyroglobulin synthesis as an indicator of early random dedifferentiation of the Fischer rat thyroid cell line FRTL-5. Scand J Clin Lab Invest 58:529–535
28. **Goretzki PE, Frilling A, Simon D, Roeher HD** 1990 Growth regulation of normal thyroids and thyroid tumors in man. Recent Results Cancer Res 118: 48–63
29. **Kogai T, Curcio F, Hyman S, Cornford EM, Brent GA, Hershman JM** 2000 Induction of follicle formation in long-term cultured normal human thyroid cells treated with thyrotropin stimulates iodide uptake but not sodium/iodide symporter messenger RNA and protein expression. J Endocrinol 167:125–135
30. **Tonacchera M, Viacava P, Agretti P, de Marco G, Perri A, di Cosmo C, de Servi M, Miccoli P, Lippi F, Naccarato AG, Pinchera A, Chiovato L, Vitti P** 2002 Benign nonfunctioning thyroid adenomas are characterized by a defective targeting to cell membrane or a reduced expression of the sodium iodide symporter protein. J Clin Endocrinol Metab 87:352–357
31. **Chun YS, Saji M, Zeiger MA** 1998 Overexpression of TTF-1 and PAX-8 restores thyroglobulin gene promoter activity in ARO and WRO cell lines. Surgery 124:1100–1105
32. **Shimura H, Suzuki H, Miyazaki A, Furuya F, Ohta K, Haraguchi K, Endo T, Onaya T** 2001 Transcriptional activation of the thyroglobulin promoter directing suicide gene expression by thyroid transcription factor-1 in thyroid cancer cells. Cancer Res 61:3640–3646
33. **Takeda T, Yamazaki M, Minemura K, Imai Y, Inaba H, Suzuki S, Miyamoto T, Ichikawa K, Kakizawa T, Mori J, DeGroot, LJ, Hashizume K** 2002 A tandemly repeated thyroglobulin core promoter has potential to enhance efficacy for tissue-specific gene therapy for thyroid carcinomas. Cancer Gene Ther 9:864–874
34. **Kanegae Y, Lee G, Sato Y, Tanaka M, Nakai M, Sakaki T, Sugano S, Saito I** 1995 Efficient gene activation in mammalian cells by using recombinant adenovirus expressing site-specific Cre recombinase. Nucleic Acids Res 23:3816–3821

THYROID
Volume 14, Number 1, 2004

Cloning of the 5′-Flanking Region of Mouse Sodium/Iodide Symporter and Identification of a Thyroid-Specific and TSH-Responsive Enhancer

Xiaoqin Lin,[1] Kwon-Yul Ryu,[2] and Sissy M. Jhiang[1]

The sodium/iodide symporter (NIS) mediates active iodide uptake into thyroid follicular cells and is important for the diagnosis and radioiodide treatment of thyroid cancers. In order to better investigate the transcriptional regulation of the NIS gene, we cloned the 3.2 kb 5′-flanking region of the mouse NIS (mNIS) gene in this study. The cloned 5′-flanking region of mNIS shares 68% identity with that of rat NIS (rNIS), yet has little similarity to that of human NIS (hNIS). Based on sequence homology to rNIS, the putative mNIS transcriptional start site is mapped to −97 nt relative to the ATG site. The minimal promoter of mNIS is located within 650 bp of the 5′-flanking region as determined by the transient expression analysis of promoter-reporter constructs. The mNIS upstream enhancer (mNUE) was identified based on sequence homology to rNUE. The mNUE is localized to the region between −3042 and −2809 nt relative to the ATG site and shares 94.4% identity with rat NUE (rNUE), while only 67.8% identity with human NUE (hNUE). It contains two Pax-8 binding sites and a Tax/CREB binding site. The mNUE is also demonstrated to confer thyroid-specific and TSH-responsive transcriptional activity. The high degree of homology in the 5′-flanking region between mNIS and rNIS suggests that mNIS and rNIS share similar mechanisms for transcriptional regulation.

Introduction

THE SODIUM/IODIDE SYMPORTER (NIS) is a transmembrane glycoprotein that mediates active iodide transport into thyroid follicular cells (1). The active iodide uptake is not only the first and rate-limiting step for thyroid hormone biosynthesis, but also the basis for the use of radioiodide (^{131}I) in diagnosis and treatment of differentiated thyroid cancers (2–5). Because of the physiologic and therapeutic significance of NIS in thyroid cells, the regulatory mechanisms underlying NIS gene expression have attracted much attention. Several groups have attempted to elucidate the transcriptional regulation of rat NIS (rNIS) and human NIS (hNIS) genes by characterizing their corresponding 5′-flanking regions (6). The minimal region for rNIS promoter activity is localized to −291 to −135 nt relative to the ATG site (7–9), while the hNIS minimal promoter is localized to −443 to −395 nt relative the ATG site (10–11). It has been shown that the NIS minimal promoter alone is not sufficient to confer thyroid-specific transcriptional activity. Among the cis-acting elements identified, the rNIS upstream enhancer (rNUE), located at −2495 to −2264 nt relative to the ATG site, represents the most important aspect of NIS gene regulation. The rNUE contains two paired domain-containing transcription factor (Pax-8) binding sites and a degenerate cAMP response element (CRE) sequence, and stimulates transcription in a thyroid-specific and thyrotropin (TSH)-cAMP-responsive manner (9). Based on sequence homology to rNUE (69% identity), the hNIS upstream enhancer (hNUE) was identified and shown to confer thyroid-specific and TSH-cAMP-responsive transcriptional activity (12–14). The 296 bp hNUE is located at −9348 to −9054 nt relative to the ATG site and contains a Pax-8 binding site and a CRE-like sequence.

Recently, mouse NIS (mNIS) cDNA was cloned and found to exhibit 92% identity with rNIS cDNA, while only 78% identity with hNIS cDNA (15–18). Using the genomic walking method, a 3.2 kb genomic DNA fragment corresponding to the 5′-flanking region of the mNIS gene was cloned and characterized. The 3.2 kb 5′-flanking region of mNIS shares 68% identity with that of rNIS, yet shares little similarity with that of hNIS. Based on sequence homology, the mNIS upstream enhancer (mNUE) was localized to the region between −3042 and −2809 nt relative to the ATG site. The mNUE shares 94.4% identity with rNUE and enhances transcription in a thyroid-specific and TSH-responsive manner.

[1]The Ohio State Biochemistry Program, Department of Physiology and Cell Biology, The Ohio State University, Columbus, OH; [2]Department of Biological Sciences, Stanford University, CA.

Materials and Methods

Cloning of 3.2 kb mNIS genomic DNA fragment

Based on the published sequence of mNIS cDNA, two mNIS gene-specific reverse primers, mNISGSP1 (5′-GCA CCT GCA CAG CCG A CA TGA AGC TA-3′) and mNISGSP2 (5′-CAG CAT GGT CGC GAA CAC GCC GTA GT-3′), were designed, corresponding to +220 to +195 nt and +72 to +47 nt relative to the putative ATG site, respectively. With these two primers and the adapter primers provided by the mouse genomeWalker™ kit (Clontech, Palo Alto, CA), PCR reactions were performed using platinum Taq DNA polymerase (Gibco, Invitrogen, Carlsbad, CA). The modified procedure of primary touchdown PCR includes 7 cycles of denaturation at 94°C for 2 seconds, annealing and extension at 70°C for 3 minutes, then 37 cycles of denaturation at 94°C for 2 seconds, annealing and extension at 65°C for 3 minutes, and finally an extension at 65°C for 4 minutes. The secondary touchdown PCR includes 5 cycles of denaturation at 94°C for 2 seconds, annealing and extension at 70°C for 3 minutes, then 24 cycles of denaturation at 94°C for 2 seconds, annealing and extension at 65°C for 3 minutes, and finally an extension step at 65°C for 4 minutes. Two DNA fragments, 1.8 kb and 3.1 kb in length, containing the 5′-flanking region of the mNIS gene were amplified from DraI and PvuII mouse genomeWalker libraries, respectively. These two DNA fragments were cloned into the TA cloning vector pCR2.1 (Invitrogen), named 1.8 kb/pCR2.1 and 3.1 kb/pCR2.1, and their nucleotide sequences were analyzed. Based on the sequence determined from the 3.1 kb DNA fragment, two reverse primers, mNISGSP3 (5′-GTG TCT AGA AGA AGG TGT TGG GCC TC-3′) and mNISGSP4 (5′-GAA GCA ATC AGT GTC CAG AGA CTG TC-3′), corresponding to −2832 to −2807 nt and −2940 to −2915 nt relative to the ATG site, respectively, were designed for another round of genomic walking. The resulting 350 bp DNA fragment from the DraI library was cloned into pCR2.1 vector to generate 350 bp/pCR2.1 for nucleotide sequence analysis.

Plasmids

1.8 kb/pGL$_2$B was constructed by inserting the 1.8 kb KpnI-EcoRV fragment from 1.8 kb/pCR2.1 vector into the Kpn1-HindIII sites of pGL$_2$B, which is a promoterless luciferase vector. The mNIS/pGL$_2$B DNA construct was subsequently generated by removing the 969 bp SpeI-MluI fragment from 1.8 kb/pGL$_2$B and then removing the putative ATG site by digesting with NcoI enzyme, followed by Mung Bean nuclease treatment (New England Biolabs).

The putative mNUE DNA fragment was amplified from mouse genomic DNA by PCR using a pair of primers, mNUE-F1 (5′-*GGT ACC* GAT TGC AGC TGG CAA GTG CC-3′) and mNUE-R1 (5′-*GAG CTC* TCT AGA AGA AGG TGT TGG GC-3′) where the italics are the KpnI and SstI sites, respectively. The resulting putative mNUE was cloned into the KpnI/SstI sites of mNIS/pGL$_2$B, generating mNUE-mNIS/pGL$_2$B.

Cell culture, transient transfection, and luciferase assay

FRTL-5 rat normal thyroid cells were cultured in Coon's modified Ham's F12 medium, supplemented with 5% calf serum and six hormone (6H) mixture containing TSH (1mU/mL), insulin (10 μg/mL), hydrocortisone (10 nM), transferrin (5 μg/mL), and L-glycyl-histidyl-lysine (2 ng/mL) (7). Rat-1 rat embryonic fibroblast cells were maintained in DMEM supplemented with 10% fetal bovine serum (FBS).

Cells were seeded in 6-well plates. When cells became 50%–60% confluent, calcium phosphate transfection was performed using 3 μg of promoter-luciferase reporter DNA construct and 0.2 μg of β-galactosidase DNA construct. The DNA precipitates were replaced with fresh medium 6 hours later for FRTL-5 cells or 20 hours later for Rat-1 cells. Cells were washed with PBS and lysed with 80 μL of the lysis buffer 48 hours post-transfection in a luciferase assay kit (Promega, Madison, WI). The luciferase and β-galactosidase assays were carried out as described previously (7). For luciferase assay, 20 μL of cell lysate was used. For β-gal assay, 7 μL of lysate was used with the Galacto-Light chemiluminescent β-galactosidase reporter assay kit (Tropix, Applied Biosystems, Foster City, CA). Experiments were performed in duplicate.

The investigation of the effects of TSH on (enhancer)/promoter constructs in FRTL-5 cells was performed as described previously (9). The transfected FRTL-5 cells were cultured in starvation medium supplemented with 0.2% calf serum for 72 hours and then incubated in the 4H medium (without insulin and TSH) or with 4H + TSH (without insulin) for an additional 72 hours. The cells were harvested, and luciferase and β-galactosidase assays were performed.

Computer-assisted identification of potential transcription binding sites in the 5′-flanking regions of NIS

Potential transcription factor binding sites in the 5′-flanking regions of mNIS, rNIS, and hNIS genes were analyzed using the MatInspector Release Professional 6.2 program (Genomatix, Munich). A core similarity, defined by the consecutive highest conserved positions in the matrix, was set to be larger than 0.8. A matrix similarity took into account all bases over the whole matrix and was set as optimized, which minimized false positives and false negatives for each individual matrix (19).

Results

Isolation and sequence analysis of the 3.2 kb mNIS 5′-flanking region

Two gene-specific primers, mNISGSP1 and mNISGSP2, were derived from the published 5′ end of the mNIS cDNA sequence (17). After one round of genomic walking, the 1.8 kb DNA fragment from the DraI library and the 3.1 kb DNA fragment from the PvuII library were obtained and sequenced. The 1.8 kb DNA fragment contains 1596 bp of mNIS 5′-flanking region and 220 bp of mNIS open reading fragment (ORF) sequence. The 3.1 kb DNA fragment contains 3012 bp of mNIS 5′-flanking region and 72 bp of mNIS ORF sequence. Another round of genomic walking using two mNISGSP3 and mNISGSP4 reverse primers based on the identified 3.1 kb mNIS promoter sequence was performed to isolate a 350 bp DNA fragment from the DraI library, which extends 233 bp further upstream of the identified mNIS 5′-flanking sequence. Taken together, 3465 bp of DNA sequence, including 3245 bp of the mNIS 5′-flanking region and 220 bp of mNIS ORF, was determined (Fig. 1). The de- F1

```
                                                    +NGNRNAWCAAAGGRNNN LEF-1
-3245                                    TAAATAGTGGTGCACACAGCAAAGGGGCTTCGTCG

                               +NNNNNTGASTCANNNNNNNNN AP1
-3210 CCTTTGGGGGGCTGTGCAGTGCCCCCCAGAGTGAATCAGTAGGCTCTACAGAATGTGGGGGCATTCTGGG
  - NCGCCNSGGGMK AP2

-3140 TGGCTGGGGCTGATTTTTTTTTTTTCTTTCCACAGACCGAGACATGGGTGCCCGACACCGTGCCCGTGCC
-NGGGGKKGTTTGGGG RREB1   -NTRTNNMTTRCMNMANWCN  CEBP
                                         -NKCACCCWTGGGTGCNN ROAZ

                                                        +NNNNCANCTGNYNNN MYOD
                                          +MMGYCGSGYGCMSSY HES1
-3070 CACTCCATCCAGATCATGAAGGTGGAAGAGATTGCAGCTGGCAAGTGCCGCCGGCCAGCTGTCAAGCAGT
                               -GGGKATTGCAYNN CHOP    -NNNNNNCAGCTGNNNNN AP4
                                                 PBX1_MEIS1 -NNCCTGTCAATCAWNNN
                                                             -ASCTGTCAN MEIS1

                                                +NNSTGTGGTTTGTGN AML3
                              +NNRWKACSCANNGNKGMGTGRCSNCNNNN PAX9
  +NNNNNCACGTGNN ARNT        +NNTGCTGACTCAGCANNNNNN VMAF
   +NNNNCACGTGNNNNN USF    +GGGGGTTGACGYANANNNNNN TAXCREB
-3000 TCCACGTGAGTGACCCCGAGTGTGGGGCTGACGCAGGGCTGCAGGGGGTGGTTGCACACGGACAGTCTCT
 -AWNNNMCACGTCANC XBP1         -NNKCACKCAWSNSTGCNNN PAX4_PD
     -NSCACGTNNGNNN HIF1                     -NNNGGGGGNGGNNNN ZBP89

-2930 GGACACTGATTGCTTCCCTCCCCACAGGACTCCAAGATCAAATTCCCACTGCCCCACCGTGTGTTGCGGC
                -NCTCCCCTCSCMN MAZ                        RFX1 -NNNNGTTRCYNNGYNACNN
                       -TCCCCNC MZF1

-2860 GCCAGCACAAGCCACGCTTCACCACCAAGAGGCCCAACACCTTCTTCTAGACACAGAGACCCACTGAATA
                                                              PIT1 -NATGAATAAWT

-2790 AAAACTTGAGACTGTCCTTGCTTGTTTGCTTTGTCCCTGGAGAGGTCCCAGTTGGTCCCGTCCCTAACAA

-2720 CATGCTAGCCCTGCTCACCTGCCTGTCAGCCTTGCTCAGTGGCATCTTTCCATAGGTGTGTATCCCCTTA
                                                     -NCNATANNTATYGGTGN CDPCR3

-2650 GATTAGCTTCAGCCCCACTACGATTTGTCTAGGACATAGCCTGAGCCCTGCCTGTGACACTGAGGGAGCA
                                       -NGWAACCTGASCM MEF3

                                            +NNNAAWKCCAGAYNCNN THIE47
    +NNNNNGTTTSNNN AREB6                  +NNNNNAGKKCCAGGNNMGN PAX6
-2580 GTCTGTTTCTGGACTCCAGGGTGCTGCGGTCTCAGGCCTAAGAATTCCAGACAGGACTATAATCCAAGCC

-2510 TGGGGATCTGGTTGAGCTTTTTATCCTGCTGGCTCTAAGCTTCAGCTAGGTGGAAATGAGGCCAGCCAAG
                     -NKNCTTATCNNNN GATA
```

FIG. 1. The transcription factor binding sites shared by both mNIS and rNIS in the 3.2 kb 5′-flanking region. The nucleotide sequence of the mNIS 5′-flanking region is shown in bold letters. The first nucleotide of the translation initiation site (ATG) is designated as +1. The arrow indicates the putative transcriptional start site. The potential TATA box is underlined. The identified potential transcription factor binding sites with their consensus sequences are shown in the upper (+) or lower (−) strand of the mNIS 5′-flanking region.

termined 220 bp mNIS ORF sequence matches the published mouse cDNA sequence. The 3.2 kb 5′-flanking region of the mNIS gene shares 68% identity with that of the rNIS gene. Higher homology regions with about 80% identity are found AU1 within the proximal and distal regions of NIS[1] 5′-flanking sequence. In contrast, the 5′-flanking region of mNIS shares little similarity with that of hNIS, except in the minimal promoter and hNUE regions. The putative transcriptional start site of mNIS is located around −97 nt upstream of the ATG site, based on sequence homology with rNIS. In comparison, the transcriptional start site of rNIS is located around −98 nt relative to the ATG site, while the transcriptional start site of hNIS has been mapped to −375 nt relative to the ATG site (7–11). A potential non-canonical TATA box (AATAAAT) is identified at −124 to −118 nt relative to the ATG site, 21 nt upstream of the putative mNIS transcriptional start site. Similarly, the TATA box is located 21 nt upstream of the putative rNIS transcriptional start site and 23 nt upstream of the putative hNIS transcriptional start site (7–11). Potential transcription factor binding sites in the 5′-flanking regions of mNIS and rNIS genes were analyzed by the MatInspector Release Professional 6.2 program. A total of 204 and 279 potential transcription factor binding sites were identified in the 3.2 kb 5′-flanking regions of rNIS and mNIS, respectively. Among these transcriptional binding sites, 63 were shared by both mNIS and rNIS. Interestingly, the MatInspector Re-

```
-2440 CCCTACAGTGAGCTTGCAAGCTTTAGATGGGGACAGGGTTACGCTTTGGTGAATGGTGGAGGAAACATGG
                  -CCNYCNGCTTTNNAT BARBIE

-2370 GGGTTCCTTTTGTTGGGTGCAGCCAGCACGGCATCATCATGGTGCCCAATCTTGAAAGGGCACAGGCCTG

-2300 AAGCTTCCTGGGACTGTTCTGTCACAGGGAGGAACCTACTGCAGTTGCCTACAATTGCTACCTCTGAGGG

-2230 ACTTTCCTCTGGCCCCTTGTAGACATTTCCATGTCTACACATGGCCCAGAGTACTTTCAGGGATAGCAAT
                         -NMKNATTTGCATAYY OCT1

-2160 TAACATGTGAATTCCAGACCAGTGAAGGTTACAAAGTCAAACCCTGTCAAAAATTGCTGTGTGTGGGTGT

                              +NNGNCCAWATAWGGMNNNNN SRF
-2090 TACAAAGCCCAAGTCTGTACGTTTGAAAACCATAAGAGGGCATCTGGTCTATAGATGATTCTTTTTCCCA
                                                           E2F  -YMRTTTTCGCSWA

                   +NNNNNWTCAAAGNNNNN LEF1
          +TRSASTGTNCMGWSSTKAAACKS PAX2
-2020 TTAAGTCCATTGGTCCCACATCAAAGGAATGGGTGATCCCTCAGACTGCATTGCTTCCCTGTGCAGAGTA
        -NNNYSATTGGYYANN NFY
                         -NCNSWGGAATGTR TEF-1

-1950 GAACCAGTGGCTGCTGCTTTGGAAACTTGAAGAATCCATGAAAAGTTCCTTCTCTTAACCTGGTTTTGTC

-1880 CCTAGCACCTGTATTAGGCCCACATCTGTAACTCTTGCTCCAGGATATCAGATGCCTCTGCAGGCGCCAG

-1810 AATTCATATACAGCTCCCCTTCACCCACGTGCATAATTAAGTTTTGTTTTGGGGAGTTTGTGAAGATACC
  -NNNAATTANCATANA OCT1               -NTAATTRNN S8
                                             -NGGGGKKGTTTGGGG RREB-1

-1740 TGGTGTGAGACTAAGCCCAGCCCTCAGGGAGGCAAAGACAGATCTGAGTTCGAGGCCATCCTGGTCTAAA

     +NNNNNAGKKCCAGGNNMGN PAX6
-1670 AGGTGAGTTCCAGGACAGTCAGGGCTACACCAAAAGAAACATTGGGTAGGCACACAACCAGCCCCAGCTC

-1600 TCCCTGAAGCTAGGCACAGGTCATGACTGCAAGTGTTGTCCCAACATGGCAGTCCCGCCTGCCTCGGGAA

-1530 GACTCTTCCCTCCCTCCTGCATTAGTGCTTCTTCCCATTCAGAATGCCTCGTACATGTGTCATCTCATCT
        -NCTCCCCTCSCMN MAZ

-1460 TAGTTCTACCCATTCTGAAGCCTTTCAAAAACCTGAAACCCCGGGCTGGAGAGATTGGCTCAGTTAAGAG

-1390 CACTGACTGCTCTTCCAGAGGTCCTGAGTTCAGTTCCCAGCAACCACAATGTGGCTCACAACCATCTGTA

-1320 ATGGAATCCAGTGCCGCCTTCTGGTGTGTCTGAAGCCAGCTACAGTGTACCCACATGTAAATATAAAATA

-1250 AAGTCTAATAAGAAGAGAAAAGCCCTTTCAACCTCATCAGTAATGCCCTCAAGCCCGCCTGCCACCTAGG

-1180 TTTAGGAGACTGCCCTAGCCAGGCCTCCCTCCTAACCAGCACCTCCAGGCAGGCAGTCCAGCCAGTATAC

                    +NNNNNNNNNNGNRCCTTNNNN MOK2
-1110 AGCATATGAGGCCACCAGGGGGCGTGTGCCTTAGTTTTACTTATCAGACCACCCGGGAGGTACAGACGTG
```

FIG. 1. *Continued.*

lease Professional 6.2 program failed to identify the two Pax-8 binding sites, which are located in the NUE region of mNIS and rNIS. This may be due to underdeveloped consensus sequences of the Pax-8 site in the software.

A stretch of 234 bp between −3042 and −2809 nt relative to the ATG site, which shares 94.4% identity with rNUE, was identified as the putative mNUE (Fig. 2). The putative mNUE also contains two Pax-8 binding sites and a cAMP response element (CRE)-like sequence based on sequence homology to rNUE. Using the MatInspector software, both mNUE and rNUE were found to contain a Tax/CREB binding site, while hNUE contains a CREB binding site (20). Thus, the sequence surrounding the CRE-like sequence is well conserved between mNUE and rNUE, yet it is completely divergent between mNUE/rNUE and hNUE.

Functional analysis of mNIS promoter and mNUE

To investigate the promoter activity of mNIS, a 650 bp DNA fragment corresponding to the immediate 5′-flanking region of mNIS was inserted into a promoterless luciferase reporter construct pGL_2B to generate mNIS/pGL_2B. To in-

```
                                                  +TWSGCGCGAAAAYKR E2F
                                +NNGNCCAWATAWGGMNNNNN SRF
                            +NNGACCACCCARNNN GLI1
-1040     GCTCAATAGGGAATCAACCCTGAACACCCAGAAACGGCTAGTTCTCCAGAAAAAGGTCCCACGGTGACAG

                                                    +NNRGNACNNKNTGTTCTNN PRE
-970      TTCTGCATCATCCCAAGCCCTGGGTCCCTTGAAAGCCACTATCAAGCAAACTTCTGTTCTGGACCCAGGT

-900      ATGCCAAAGTACCTGCGACAAGAAGGGAGAAATGGGTATTCAATGAACCCTCACTTGTCATCCCAGCACT

-830      AGGGAAGCCATGGCAGGATTGACACACCTTTGTGATCAGCCTGTGGGAAAGAAAGGAAGAGAACAGGAAA

-760      GGGGAAGACAGCCAGGTCAGGTGTAGTGCACACTCTTGTGTTCCTGCCGGTAGGGTGGGCCTTGGTCAGG

-690      ACTCCATACCAGCCTGAGCTACATGAGACTCAGCCTCAAACGCGTGCGTACACGCATACACACACACACA

-620      CACACACACATACAACCATAGGTCCAGACTGCCCTGTGCAGGTAGGGAAACTGAGTCCTAAACAGAAGGA

      +NNNRNRAATTTNCSNNN HMGIY
-550      AGAAATTCTCCAAAGAGAACCTGAGTGCCTCCCACCGGGTTAGCAAGGGTGGACAGTTCCTTCTCCCACG
                                                          -NNNYMASTTCCTSYWNN PU1

                                                          CETS1P54 +NNNNCMGGAWGYNNNNN
-480      CTGCGGAGAAAGGCAGATGCTCTCTCGGGGGAAGGCTCGAGTCTCGTTTTTCCTTATGGGGCCCGGAAGT
                                                   -NNNNTTTTTSC NMP4
                                                      -NNTTTTCCWNN NFAT

           +NNGAAWNYGAAANTN IRF7
-410      CCCCGAAAGTGAACCCCAGTCCCGGGTTCCTCGTAGCTTCGGTTCCTAACTCCCGCAGGCTGTGTGAACA

-340      GAGGGGAGCGGAGGTCTGAGCCGTCCAAGGCCCTTCCCGTCTGTCCACAACTCTACACGGAACAAGCCCT

-270      AGATGTGGGAGAAAGTGTCAGGAGACGCTAGTGTCCCCCAACCCCGTTGCCCGCACCCCTGAAGGCCCGC
                                                      -SNCGCSCCCACNCNN WT1

                    +CNSNNAGGGTN EKLF
       +GCNMNAMCMAG CP2                                     VMAF +NNTGCTGACTCAGCANNNNNN
-200      TCGCCCCAGGACGGAAAGGGTGCGGGTCGCGCCCGCCTCCCAGGCTGTGGGCGGGGCCGCGCTGACCCCG
                       -NNNRGGGGYGGSNYC ZF9
                                  -NNNGCGCNCAC ZF5
                                       -NCTCCCCTCSCMN MAZ

-130      GAGCCCAATAAATCCGCCGCGCGAAAAGCTAGTGGGTCGACGGCCCAGCAGGGACTCGCGCAGCGACGAC
               TATA box                    ↑
                                                                      +1
-60       GCTCTCTCTGAGAGTCCCCGACGTCCTCCGCATCCTCTCCGTTCCGAGTCACCTGTCTCC ATG GAG GGC

          GCG GAG GCA GGG GCC CGG GCC ACC TTC GGC CCC TGG GAC TAC GGC GTG TTC GCG
          ACC ATG CTG CTG GTG TCC ACG GGC ATC GGT CTG TGG GTC GGC CTG GCC CGC GGC
          GGC CAG CGC AGC GCC GAC GAC TTC TTC ACC GGG GGC CGG CAG CTG GCG GCA GTG
          CCT GTG GGG CTG TCG CTG GCC GCT AGC TTC ATG TCG GCT GTG CAG GTG C
```

FIG. 1. *Continued.*

vestigate the functionality of the mNUE, a 233 bp of PCR-amplified DNA fragment corresponding to the putative mNUE was inserted into mNIS/pGL$_2$B to generate mNUE-mNIS/pGL$_2$B. The promoter activities of these two DNA constructs were evaluated in the FRTL-5 rat thyroid cells and the Rat-1 rat fibroblast cells. As shown in Fig. 3, mNIS/pGL$_2$B conferred significant promoter activity in both thyroid and non-thyroid cells, compared to the promoterless pGL$_2$B. Thus the minimal promoter of mNIS is located within the 650 bp of the 5′-flanking region, and the minimal promoter activity is not thyroid-specific. We also showed that the enhancer activity of mNUE is thyroid-specific, as mNIS promoter activity was increased by mNUE more than threefold in FRTL-5 thyroid cells but not in Rat-1 fibroblasts. To determine whether the enhancer activity of mNUE is TSH responsive, mNIS/pGL$_2$B and mNUE-mNIS/pGL$_2$B DNA constructs were transfected into FRTL-5 thyroid cells in the absence or presence of TSH. The enhancer activity of mNUE on mNIS promoter activity was dramatically stimulated by TSH (almost eightfold) (Fig. 4). In contrast, TSH did not increase luciferase activity of cells transfected with mNIS/pGL$_2$B.

F3

F4

Discussion

NIS expression in thyroid tissues is not only of physiologic significance but also of clinical significance. While some thyroid cancers have defects in NIS cell surface trafficking (5), many thyroid tumors have decreased NIS expression. Studying the mechanisms underlying NIS regulation in thy-

```
                                            Pax-8 binding site
-3042 AGATTGCAGCTGGCAAGTGCCGCCGGCCAGCTGTCAAGCAGTTCCACGTGAGTGACCCCGAG--------
      ::::::::::::::::::::::::::::::::::::::::::::::::::::::: :: :::
-2495 AGATTGCAGCTGGCAAGTGCCGCCGGCCAGCTGTCAAGCAGTTCCACGTGAGTGAACCTGAG--------
      :::: :: ::  ::::::::::::::: :::::::::::::::::::::::  :::: :
-9339 AGATCGCGGCCAGCAAGTGCCGCCGGCCGGCTGTCAAGCAGTTCCACGTGAGTGC-CCTGGGGACTCCC
                                            Pax-8 binding site

          Tax/CREB +GGGGGTTGACGYANANNNNNN          Pax-8 binding site
-2980 -TGTGGGG-----------CTGACGCAGG---GCTGCAGGGGGTGGTTGCACACGGACAGTCTC------
       :::::::           ::::::::::   ::::::::::::::::: :: :::::::: :
-2433 -TGTGGGG-----------CTGACGCAGG---GCTGCAGGGGGTGGTTGCGCATGGACAGTCCC------
       ::  :::           ::::::::::     : :  ::::: :: : : : : :   : :::
-9270 CTGGAGGGAAGTGCCTGCTCTGACGCAGGAGCCCAGTGGGGGGCGGCTACACCTTGGTGGCCCCACAGGA
              CREB +NNNNNSTGACGTAANNNNNNN

-2931 TGG-------ACACTGATTG---------------CTTCCCT-CCCCACAGGACTCCAAGATCAAATTCC
      :::       :::   ::                : ::::: ::::::::::::::::::::: ::::
-2384 TGG-------ACATGCATCT---------------CCTCCCT-CCCCACAGGACTCCAAGATCAAGTTCC
      :::       : : :: ::                ::::::: :: ::::::::::::::::::::::
-9200 TGGGGTGTTAAGAGGCTTCCAACCCCCTCAACATGCCTCCCTTCCTCACAGGACTCCAAGATCAAGTTCC

-2884 CAACTGCCCCACCGTGTGTTGCGGCGCCAGCACAAGCCACGCTTCACCACCAAGAGGCCCAACACCTTCT
      ::: :::::::::::::::::::::::::::::::::::::::::::::::::::::: :::::::::
-2337 CAATTGCCCCACCGTGTGTTGCGGCGCCAGCACAAACCACGCTTCACCACCAAGAGGCCAAACACCTTCT
      :   ::::::::: ::  ::::::: ::::::: :::::::::::::::::::::::: :::::::::
-9130 CGGCTGCCCCACCGGGTCCTGCGCCGTCAGCACAAGCCACGCTTCACCACCAAGAGGCCCAACACCTTCT

-2814 TCTAGA  mNUE
      ::::::
-2267 TCTAGA  rNUE
      :::::
-9060 TCTAGG  hNUE
```

FIG. 2. Sequence alignment among mNUE (upper), rNUE (middle), and hNUE (bottom); 234 bp of mNUE is highly conserved with 234 bp of rNUE (94.4% identity), while mNUE shares 67.8% identity with 285 bp of hNUE. The Pax-8 and CREB sites are underlined.

roid tissue will help to devise strategies for increasing or restoring ^{131}I-concentrating activity in thyroid cancers, allowing effective ^{131}I therapy. Furthermore, most factors affecting iodide uptake activity in thyroid tissues appear to regulate NIS expression at the transcriptional level (6). Since the mouse is a useful preclinical animal model to screen for important factors that increase NIS expression in thyroid tissues, we cloned and characterized the 3.2 kb 5′-flanking region of mNIS in this study. The 3.2 kb 5′-flanking region of mNIS shares 68% identity with that of rNIS, yet shares little similarity with the corresponding region of hNIS. Based on sequence homology to rNIS, the putative mNIS transcriptional start site is mapped to −97 nt relative to the ATG site, in contrast to −375 nt in hNIS. Furthermore, mNUE, localized to the region between −3042 and −2809 nt relative to the ATG site, shares higher homology with rNUE (94.4% identity) than with hNUE (67.8% identity). Finally, we demonstrated that mNUE enhances mNIS transcription in a thyroid-specific and TSH-responsive manner.

Despite their sequence divergence, both hNUE and rNUE activities require a CRE-like sequence and Pax-8 binding sites (9,12–14). However, rNUE can be activated by exogenous Pax-8 in both thyroid and non-thyroid cells (9), while hNUE can only be activated by exogenous Pax-8 in thyroid cells (12–13). It is of interest to note that hNUE contains only one Pax-8 binding site, yet both rNUE and mNUE contain two Pax-8 binding sites. Thus, the second Pax-8 binding site may play an important role in activating rNUE activity in non-thyroid cells. It is also important to note that while both the sequence surrounding the CRE-like sequence and the transcription factors binding to the CRE-like sequence appear to be very different between hNUE and r/mNUE (9, 13–14), the NUE in all three species exerts enhancer activity in a thyroid-specific and TSH-responsive manner. Based on sequence homology to rNUE, we anticipate that mNUE can also be activated in non-thyroid cells by exogenous Pax-8 and the transcription factors binding to the CRE-like sequence of mNUE may be similar to those for rNUE.

Among the common 63 transcriptional binding sites identified in the 5′-flanking region of rNIS and mNIS, several are of particular interest. The concurring increase in AP2 expression and decrease in NIS expression in thyroid tumors suggests that AP2 may play a role in downregulating NIS expression in thyroid tumors (21). In v-ras-Ki transformed thyroid cells, NIS expression was significantly decreased (22), while AP1 activity was drastically increased (23). Thus, AP1 may be involved in downregulating NIS expression. Since Maf nuclear oncoprotein recognizes sequences related to an AP1 site and forms heterodimers with both Fos and Jun (24), Maf may have a regulatory role in NIS expression. RREB-1 has been reported to play a role in Ras and Raf signal transduction in medullary thyroid cancer cells (25). Con-

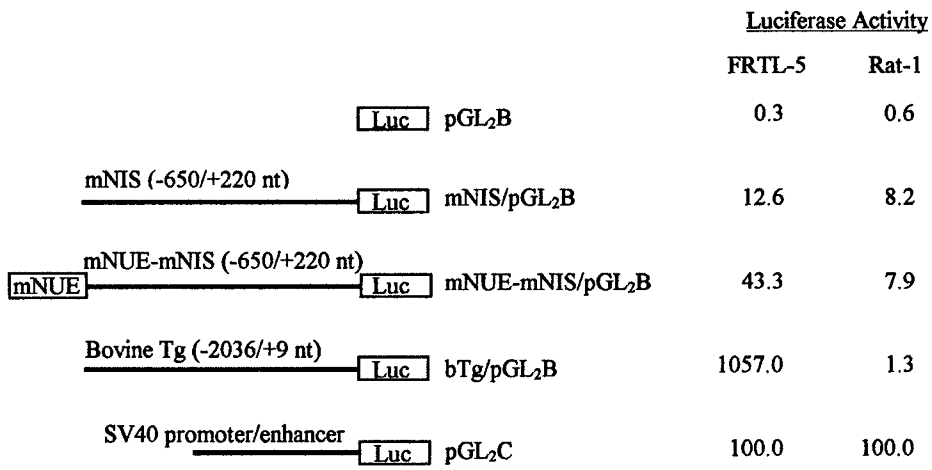

FIG. 3. Functional analysis of mNIS promoter activity. Luciferase activity of each DNA construct was determined in FRTL-5 cells or Rat-1 cells. A β-gal construct was co-transfected to normalize the transfection efficiency. The normalized luciferase activity of pGL$_2$-Control (pGL$_2$C) containing the simian virus 40 (SV40) enhancer and promoter was arbitrarily designated as 100 in each cell line. All numbering of the NIS DNA fragment is relative to the ATG site. The numbering of the bovine Tg promoter is relative to its transcriptional start site. The data represent two independent experiments. Duplicate transfections were performed in each experiment.

sidering that both Ras and Raf transformed thyroid cells had very low level of NIS expression (22), RREB-1 may be involved in NIS regulation. Because a USF binding site is colocalized with the Pax-8 binding sites identified in hNUE, mNUE, and rNUE, USF may compete with Pax-8 for binding, therefore suppressing NIS expression in thyroid cells. Indeed, the binding of USF to E-box element (CACGTG) was increased by TGF-β1 (personal communication with Dr. Leonard Kohn, NIH), and TGF-β1 has been shown to suppress NIS expression (26,27). The thyroid hormone triiodothyronine (T$_3$) was shown to decrease NIS expression in FRTL-5 cells (28). It has also been shown that T$_3$ decreases alpha-fetoprotein mRNA in HepG2 hepatoma cells by binding to the CEBP-like site (29). Thus, the CEBP binding site may play a role in T$_3$-mediated NIS expression. Oct-1 directly interacts with retinoid X receptor (RXR) and reduces the binding of heterodimer of thyroid hormone receptor/RXR to the thyroid hormone responsive element (30). Since retinoic acid (RA) has been shown to increase NIS expression in human follicular carcinoma cells and MCF-7 human breast carcinoma cells (31,32), Oct-1 may play a role in RA- or T3-mediated NIS expression. Interferon γ (IFN-γ) has been reported to exert an inhibitory effect on TSH-cAMP mediated NIS expression (33). Since interferon regulatory factor 7 (IRF-7) is induced by IFN-γ (34), the IRF-7 site may also be worthy of investigation. Taken together, AP2, AP1, v-Maf,[2] RREB-1, USF, CEBP, Oct-1, and IRF-7 binding sites may play a role in the transcriptional regulation of NIS. The investi-

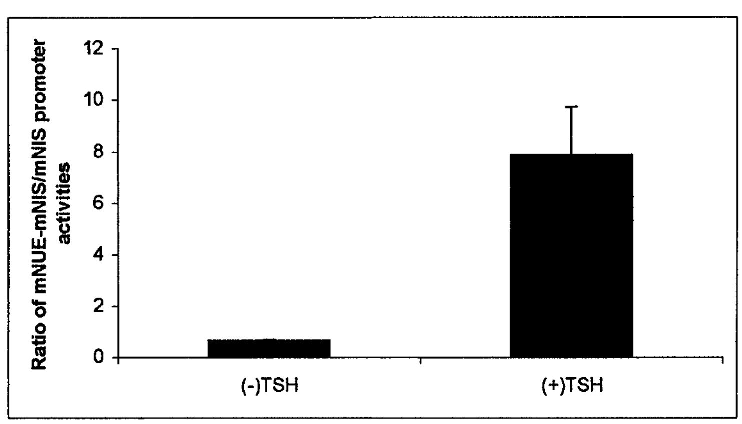

FIG. 4. The enhancer activity of mNUE is TSH-responsive. FRTL-5 cells were transfected with luciferase reporter DNA constructs containing mNIS or mNUE-mNIS. The transfected cells were cultured in the absence of TSH for 72 hours and then continued to be cultured in medium with or without TSH for an additional 72 hours. A β-gal construct was co-transfected to normalize the transfection efficiency. The data represent two independent experiments. Duplicate transfections were performed in each experiment.

gation of these factors may better elucidate the mechanisms underlying the transcriptional regulation of NIS gene.

References

1. Taurog A 1996 Hormone synthesis: thyroid iodine metabolism. In: Braveman LE, Utiger RD (eds.) The thyroid: a fundamental and clinical text. Lippincott-Raven, New York, pp. 47–81.
2. Filetti S, Bidart JM, Arturi F, Caillou B, Russo D, Schlumberger M 1999 Sodium/iodide symporter: a key transport system in thyroid cancer cell metabolism. Eur J Endocrinol **141**:443–457.
3. De La Vieja A, Dohan O, Levy O, Carrasco N 2000 Molecular analysis of the sodium/iodide symporter: impact on thyroid and extrathyroid pathophysiology. Physiol Rev **80**:1083–1105.
4. Chung JK 2002 Sodium iodide symporter: its role in nuclear medicine. J Nucl Med **43**:1188–1200.
5. Dohan O, De la Vieja A, Paroder V, Riedel C, Artani M, Reed M, Ginter CS, Carrasco N 2003 The sodium/iodide symporter (NIS): characterization, regulation, and medical significance. Endocr Rev **24**:48–77.
6. Jhiang SM 2000 Regulation of sodium/iodide symporter. Rev Endocr Metab Disord **1**:205–215.
7. Tong Q, Ryu KY, Jhiang SM 1997 Promoter characterization of the rat $Na+/I^-$ symporter gene. Biochem Biophys Res Commun **239**:34–41.
8. Endo T, Kaneshige M, Nakazato M, Ohmori M, Harii N, Onaya T 1997 Thyroid transcription factor-1 activates the promoter activity of rat thyroid Na+/I− symporter gene. Mol Endocrinol **11**:1747–1755.
9. Ohno M, Zannini M, Levy O, Carrasco N, Di Lauro R 1999 The paired-domain transcription factor Pax-8 binds to the upstream enhancer of the rat sodium/iodide symporter gene and participates in both thyroid-specific and cyclic-AMP-dependent transcription. Mol Cell Biol **19**:2051–2060.
10. Ryu KY, Tong Q, Jhiang SM 1998 Promoter characterization of the human Na+/I− symporter. J Clin Endocrinol Metab **239**:34–41.
11. Behr M, Schmitt TL, Espinoza CR, Loos U 1998 Cloning of a functional promoter of the human sodium/iodide-symporter gene. Biochem J **331**:359–363.
12. Schmitt TL, Espinoza CR, Loos U 2001 Transcriptional regulation of the human sodium/iodide symporter gene by Pax-8 and TTF-1. Exp Clin Endocrinol Diabetes **109**:27–31.
13. Taki K, Kogai T, Kanamoto Y, Hershman JM, Brent GA 2002 A thyroid-specific far-upstream enhancer in the human sodium/iodide symporter gene requires Pax-8 binding and cyclic adenosine 3′, 5′-monophosphate response element-like sequence binding proteins for full activity and is differentially regulated in normal and thyroid cancer cells. Mol Endocrinol **16**:2266–2282.
14. Schmitt TL, Espinoza CR, Loos U 2002 Characterization of a thyroid-specific and cyclic adenosine monophosphate-responsive enhancer far upstream from the human sodium iodide symporter gene. Thyroid **12**:273–279.
15. Dai G, Levy O, Carrasco N 1996 Cloning and characterization of the thyroid iodide transporter. Nature **379**:458–460.
16. Smanik PA, Liu Q, Furminger TL, Ryu K, Xing S, Mazzaferri EL, Jhiang SM 1996 Cloning of the human sodium iodide symporter. Biochem Biophys Res Commun **226**: 339–345.
17. Perron B, Rodriguez AM, Leblanc G, Pourcher T 2001 Cloning of the mouse sodium iodide symporter and its expression in the mammary gland and other tissues. J Endocrinol **170**:185–196.
18. Pinke LA, Dean DS, Bergert ER, Spitzweg C, Dutton CM, Morris JC 2001 Cloning of the mouse sodium iodide symporter. Thyroid **11**:935–939.
19. Quandt K, Frech K, Karas H, Wingender E, Werner T 1995 MatInd and MatInspector: New fast and versatile tools for detection of consensus matches in nucleotide sequence data. Nucleic Acids Research **23**:4878–4884.
20. Paca-Uccaralertkun S, Zhao LJ, Adya N, Cross JV, Cullen BR, Boros IM, Giam CZ 1994 In vitro selection of DNA elements highly responsive to the human T-cell lymphotropic virus type I transcriptional activator, Tax Mol Cell Biol **14**:456–462.
21. Chiefari E, Brunetti A, Arturi F, Bidart JM, Russo D, Schlumberger M, Filetti S 2002 Increased expression of AP2 and Sp1 transcription factors in human thyroid tumors: a role in NIS expression regulation? BMC Cancer **2**:35.
22. Trapasso F, Iuliano R, Chiefari E, Arturi F, Stella A, Filetti S, Fusco A, Russo D 1999 Iodide symporter gene expression in normal and transformed rat thyroid cells. Eur J Endocrinol **140**:447–451.
23. Battista S, de Nigris F, Fedele M, Chiappetta G, Scala S, Vallone D, Pierantoni GM, Mega T, Santoro M, Viglietto G, Verde P, Fusco A, Megar T 1998 Increase in AP-1 activity is a general event in thyroid cell transformation in vitro and in vivo. Oncogene **17**:377–385.
24. Kataoka K, Noda M, Nishizawa M 1994 Maf nuclear oncoprotein recognizes sequences related to an AP-1 site and forms heterodimers with both Fos and Jun. Mol Cell Biol **14**:700–712.
25. Thiagalingam A, De Bustros A, Borges M, Jasti R, Compton D, Diamond L, Mabry M, Ball DW, Baylin SB, Nelkin BD 1996 RREB-1, a novel zinc finger protein, is involved in the differentiation response to Ras in human medullary thyroid carcinomas. Mol Cell Biol **16**:5335–5345.
26. Pekary AE, Hershman JM 1998 Tumor necrosis factor, ceramide, transforming growth factor-beta-1, and aging reduce Na+/I− symporter messenger ribonucleic acid levels in FRTL-5 cells. Endocrinology **139**:703–712.
27. Kawaguchi A, Ikeda M, Endo T, Kogai T, Miyazaki A, Onaya T 1997 Transforming growth factor-beta-1 suppresses thyrotropin-induced Na+/I symporter messenger RNA and protein levels in FRTL-5 rat thyroid cells. Thyroid **7**:789–794.
28. Spitzweg C, Joba W, Morris JC, Heufelder AE 1999 Regulation of sodium iodide symporter gene expression in FRTL-5 rat thyroid cells. Thyroid **9**:821–830.
29. Caturla M, Van Reeth T, Dreze P, Szpirer J, Szpirer C 1997 The thyroid hormone down-regulates the mouse alpha-foetoprotein promoter. Mol Cell Endocrinol **135**:139–145.
30. Kakizawa T, Miyamoto T, Ichikawa K, Kaneko A, Suzuki S, Hara M, Nagasawa T, Takeda T, Mori J, Kumagai M, Hashizume K 1999 Functional interaction between Oct-1 and retinoid X receptor. J Biol Chem **274**:19103–19108.
31. Schmutzler C, Winzer R, Meissner-Weigl J, Kohrle J 1997 Retinoic acid increases sodium/iodide symporter mRNA levels in human thyroid cancer cell lines and suppresses expression of functional symporter in nontransformed FRTL-5 rat thyroid cells. Biochem Biophys Res Commun **240**:832–838.
32. Kogai T, Schultz JJ, Johnson LS, Huang M, Brent GA 2000 Retinoic acid induces sodium/iodide symporter gene expression and radioiodide uptake in the MCF-7 breast cancer cell line. Proc Natl Acad Sci USA **97**:8519–8524.

33. Ajjan RA, Watson PF, Findlay C, Metcalfe RA, Crisp M, Ludgate M, Weetman AP 1998 The sodium iodide symporter gene and its regulation by cytokines found in autoimmunity. J Endocrinol **158**:351–358.
34. Andrews HN, Mullan PB, McWilliams S, Sebelova S, Quinn JE, Gilmore PM, McCabe N, Pace A, Koller B, Johnston PG, Haber DA, Harkin DP 2002 BRCA1 regulates the interferon gamma-mediated apoptotic response. J Biol Chem **277**: 26225–26232.

Address reprint requests to:
Sissy M. Jhiang
The Ohio State University
Department of Physiology and Cell Biology
304 Hamilton Hall
1645 Neil Avenue
Columbus, OH 43210

E-mail: Jhiang.1@osu.edu

LIN

AU1
is “NIS” correct, or should it be “rNIS”?

AU 2
previous mention was of “Maf.” Should it be “v-Maf” throughout?